

# A Tsunami Forecast Model for Daytona Beach, Florida

Hongqiang Zhou<sup>1,2</sup> and NCTR

1. NOAA Center for Tsunami Research, Pacific Marine Environmental Laboratory, Seattle, WA
2. Joint Institute for the Study of the Atmosphere and Ocean, Seattle, WA

## Contents

<b>1</b>	<b>Background and Objectives</b>	<b>5</b>
<b>2</b>	<b>Forecast Methodology</b>	<b>5</b>
<b>3</b>	<b>Model Development</b>	<b>6</b>
3.1	Forecast area . . . . .	7
3.2	Digital elevation models . . . . .	7
3.3	Grid setup . . . . .	8
<b>4</b>	<b>Model Testing</b>	<b>9</b>
4.1	Accuracy . . . . .	9
4.2	Stability . . . . .	10
<b>5</b>	<b>Conclusions</b>	<b>10</b>
<b>A</b>	<b>Model *.in files for Daytona Beach, FL</b>	<b>28</b>
A.1	Reference model *.in file . . . . .	28
A.2	Forecast model *.in file . . . . .	28
<b>B</b>	<b>Propagation Database: Atlantic Ocean Unit Sources</b>	<b>29</b>
<b>C</b>	<b>Forecast Model Testing</b>	<b>37</b>
C.1	Purpose . . . . .	37
C.2	Testing procedure . . . . .	37
C.3	Results . . . . .	38

## List of Figures

1	Aerial view of Daytona Beach, Florida. . . . .	14
2	Transect of bathymetry along 29.2°N latitude. . . . .	15
3	Extents of A- and B-grids in Daytona Beach, Florida reference and forecast models. . . . .	16
4	Topography and bathymetry of C-grids in the reference and forecast models.	17
5	Map of the Atlantic Ocean showing the unit sources in synthetic tsunami scenarios. . . . .	18
6	Model results for the synthetic scenario of ATSZ 38-47. The upper panels show the distribution of maximum water surface elevations. The lower panel shows the time series of water surface elevations at the reference point. . . .	19
7	Model results for the synthetic scenario of ATSZ 48-57. The upper panels show the distribution of maximum water surface elevations. The lower panel shows the time series of water surface elevations at the reference point. . . .	20
8	Model results for the synthetic scenario of ATSZ 58-67. The upper panels show the distribution of maximum water surface elevations. The lower panel shows the time series of water surface elevations at the reference point. . . .	21
9	Model results for the synthetic scenario of ATSZ 68-77. The upper panels show the distribution of maximum water surface elevations. The lower panel shows the time series of water surface elevations at the reference point. . . .	22
10	Model results for the synthetic scenario of ATSZ 82-91. The upper panels show the distribution of maximum water surface elevations. The lower panel shows the time series of water surface elevations at the reference point. . . .	23
11	Model results for the synthetic scenario of SSSZ 1-10. The upper panels show the distribution of maximum water surface elevations. The lower panel shows the time series of water surface elevations at the reference point. . . . .	24
12	Model results for the synthetic scenario of ATSZ B52. The upper panels show the distribution of maximum water surface elevations. The lower panel shows the time series of water surface elevations at the reference point. . . . .	25
B1	Atlantic Source Zone unit sources. . . . .	30
B2	South Sandwich Islands Subduction Zone. . . . .	35
C1	Testing results from the forecast model in scenario ATSZ 38-47: maximum water surface elevations in A-grid (a), B-grid (b), and C-grid (c), as well as time-series at the warning point (d). . . . .	40
C2	Testing results from the forecast model in scenario ATSZ 48-57: maximum water surface elevations in A-grid (a), B-grid (b), and C-grid (c), as well as time-series at the warning point (d). . . . .	41
C3	Testing results from the forecast model in scenario SSSZ 1-10: maximum water surface elevations in A-grid (a), B-grid (b), and C-grid (c), as well as time-series at the warning point (d). . . . .	42

## List of Tables

1	MOST setup of the reference and forecast models for Daytona Beach, Florida.	26
2	Synthetic tsunami scenarios employed to test the Daytona Beach, Florida reference and forecast models. . . . .	27
B1	Earthquake parameters for Atlantic Source Zone unit sources. . . . .	31
B2	Earthquake parameters for South Sandwich Islands Subduction Zone unit sources. . . . .	36
C1	Run time of the Daytona Beach, Florida forecast model. . . . .	43
C2	Table of maximum and minimum amplitudes (cm) at the Daytona Beach, Florida warning point for synthetic and historical events tested using SIFT 3.2 and obtained during development. . . . .	44

**Abstract** This report documents the development, validation, and stability testing of a tsunami forecast model for Daytona Beach, Florida. The model is to be integrated into NOAA's Short-term Inundation Forecast of Tsunamis (SIFT) system. In this system, the tsunami propagation in nearshore waters and runup on land are simulated in real time with the numerical code of Method of Splitting Tsunami (MOST) in 3 nested grids of successively increased resolutions. The innermost grid of the present model covers the at-risk area of Daytona Beach at a spatial resolution of approximately 45 m. For the forecast of a tsunami event, the model accomplishes a simulation of 12 hours within 40 minutes of CPU time. A Reference Inundation Model using grids of higher resolutions is also constructed. Good accuracy and stability of the forecast model are observed in the simulations of synthetic tsunami scenarios.

## 1 Background and Objectives

The National Oceanic and Atmospheric Administration (NOAA) Center for Tsunami Research (NCTR) at the NOAA Pacific Marine Environmental Laboratory has developed a tsunami forecasting capability for operational use by NOAA's two Tsunami Warning Centers located in Hawaii and Alaska (Titov et al., 2005). The system, termed Short-term Inundation Forecast of Tsunamis (SIFT), is designed to efficiently, accurately, and quickly provide basin-wide warning of approaching tsunami waves. The SIFT system combines real-time tsunami event data with numerical models to produce estimates of tsunami wave arrival time and amplitudes at coastal communities of interest. This system integrates several key components: deep-ocean observations of tsunamis in real time, a basin-wide pre-computed propagation database of water level and flow velocities based on potential seismic unit sources, an inversion algorithm to refine the tsunami source based on deep-ocean observations during an event, and inundation forecast models run in real time and at high resolutions for selected coastal communities.

The City of Daytona Beach is located on the east coast of Florida. According to the 2010 U.S. Census data, this city has a population of 61,005. Daytona Beach is a principal city of the Deltona-Daytona Beach-Ormond Beach metropolitan area, where over 500,000 residents live. The mild climate of Daytona Beach makes it a year-round family-friendly attraction. Every year, this city attracts more than 8 million tourists. There are several, very large racing events held at Daytona Beach throughout the calendar year.

Daytona Beach is subject to tsunami hazards caused by earthquakes around the Atlantic Basin, especially those along the eastern edge of the Caribbean Plate and the eastern edge of the Scotia Plate. The city was hit by a small tsunami that was triggered by an Mw 8.1 earthquake off the northeast coast of the Dominican Republic. Another small tsunami impacted this area 4 days later as a result of a major aftershock offshore the Dominican Republic. Besides earthquakes, submarine and subaerial landslides may also trigger tsunamis that pose a threat to the U.S. east coast cities, including Daytona Beach (e.g., Driscoll et al., 2000; Ten Brink et al., 2008; Løvholt et al., 2008; Zhou et al., 2011). Tsunamis may also be triggered by other uncommon causes and bring considerable damage to this area. On July 3-4, 1992, a long wave approximately 3 m high, reported to be forced by a propagating squall line, impacted Daytona Beach and caused significant runup on land (Churchill et al., 1995).

## 2 Forecast Methodology

The main objective of a forecast model is to provide a quick and accurate estimate of the tsunami arrival time, wave heights, and inundation during a tsunami event. All the models are designed and tested to perform under stringent time constraints, given that time is generally the single limiting factor in saving lives and property. A forecast model relies on a high-resolution numerical model, which simulates the nearshore propagation and coastal runup in real time. The numerical model employs the Method of Splitting Tsunami (MOST), which solves the shallow water equations through a finite difference scheme. MOST has been extensively validated against laboratory experiments (Synolakis et al., 2008), as well as historical tsunami events (Wei et al., 2008; Tang et al., 2008). The numerical model is run

in 3 nested grids at successively increased resolutions to gradually zoom a simulation into the population and economic center of a community of interest. The high-resolution grids are constructed based on the digital elevation models (DEMs) developed by the National Geophysical Data Center (NGDC) and NCTR. Readers are referred to Titov and González (1997) for the technical aspects of forecast model development, validation, and stability testing and Tang et al. (2009) for the details of forecast methodology.

Simulating the tsunami propagation in an ocean basin is very time-consuming. Instead of real-time simulation, the oceanic propagation is estimated through the linear combination of tsunami source functions. A tsunami source function is the time series of water surface elevations and water velocities in an ocean basin due to a unit earthquake source, which measures  $100 \times 50 \text{ km}^2$  in area and has a slip value of 1 m, equivalent to a moment magnitude of 7.5 Mw (Gica et al., 2008). A subduction zone in the ocean basin is split into numerous unit earthquake sources. The tsunami source function for each unit earthquake source is pre-computed and stored in the tsunami propagation database. Given that the tsunami evolution in deep ocean is a linear process, a tsunami scenario can be accurately represented through the linear combination of related source functions. During a tsunami event, as the tsunami waves propagate across the ocean and successively reach DART (“Deep-Ocean Assessment and Reporting of Tsunamis”) observation sites, recorded sea level is ingested into the tsunami forecast application in near real-time and incorporated into an inversion algorithm to produce an improved estimate of the tsunami source (Percival et al., 2009).

In nearshore waters, nonlinear effects become stronger in the tsunami evolution process, and so they are simulated in real time with the nonlinear shallow water theory. A tsunami forecast model consists of 3 nested grids, named A, B, and C-grids, with successively finer resolutions. The outermost A-grid provides a smooth transition from the propagation database to the nearshore real-time simulation. The A-grid covers a large domain with offshore boundaries extended into deep ocean. During a tsunami event, synthetic boundary conditions are obtained along the open boundaries of A-grid through the linear combination of water surface elevations and water velocities in the propagation database. The innermost C-grid covers the population and economic center of the at-risk community. Due to shoaling effects, the waves become short when they approach shorelines and runup on the land. High resolution is needed for the C-grid to sufficiently represent the bathymetric and topographic features, as well as to maintain accuracy in the computational results.

The forecast models, including that of Daytona Beach, are constructed for at-risk coastal communities on Pacific and Atlantic coastlines. Previous and present development of forecast models in the Pacific region have validated the accuracy and efficiency of each forecast model currently implemented in the real-time tsunami forecast system (Titov et al., 2005; Titov, 2009; Tang et al., 2008; Wei et al., 2008).

### **3 Model Development**

Accurate forecasting of tsunami impact on a coastal community largely relies on the accuracy of the bathymetric and topographic data. The basis for the development of the grids in a tsunami forecast model is the high-resolution DEMs. For each community, the DEMs are compiled from a variety of most recent data sources. All these data have been shifted to the World Geodetic System 1984 horizontal datum, and the vertical datum of Mean High

Water. A high-resolution “reference” model is first developed. An “optimized” model is then constructed by downgrading the resolutions and reducing the domain coverage of the reference model grids. The purpose of this optimization is to reduce the required CPU time to an operationally specified period. This operationally developed model is referred to as the optimized tsunami forecast model, or simply the “forecast model”. In the development of a forecast model, the computational results are carefully compared between the forecast and reference models to make sure that due accuracy is maintained in the forecast model.

### 3.1 Forecast area

Figure 1 shows an aerial view of Daytona Beach area. The Halifax River goes through the city and splits it into two parts, which are connected through 4 bridges over the river. Due to its flat and low-lying terrain, the shore part is extremely vulnerable to floods from the ocean. The soil near the shoreline is mostly sandy. In 2004, Hurricane Frances passed the Daytona Beach area and caused severe erosion to an 11-mile segment of beach. Daytona Beach has been in the path of several hurricanes in the recent decades. It is especially important to employ the newest available bathymetry and topography dataset in the development and upgrade of the tsunami forecast model in this area.

Figure 2 presents a transect going through Daytona Beach along 29.2°N latitude. East of the coast, the water depth first increases slowly to around 100 m over a distance of more than 50 km seaward. The seabed then drops abruptly to a depth of around 800 m, and becomes mild again for nearly 250 km until it reaches the edge of the deep ocean. The abrupt variation of bathymetry may introduce significant shoaling effects to the incoming waves, when the wave height increases sharply and wavelength becomes shorter. The wide area of shallow water serves as a natural barrier, which effectively mitigates the tsunami wave height and delays the arrival.

### 3.2 Digital elevation models

The bathymetry and topography used in the development of this forecast model was based on a DEM provided by NGDC and the author considers it to be an adequate representation of the local topography and bathymetry. As new DEMs become available, forecast models will be updated and report updates will be posted at “[http://nctr.pmel.noaa.gov/forecast\\_reports](http://nctr.pmel.noaa.gov/forecast_reports)”.

The bathymetric and topographic data of the grids in Daytona Beach forecast and reference models are derived from 3 DEMs. The vertical datum of all these DEMs is set to the Mean High Water. An Atlantic basin one-minute bathymetric grid covers most of the Atlantic basin between 72°S and 72°N latitudes and 20°E to 105°W longitudes. This grid was composed by using the one-minute General Bathymetric Chart of the Ocean, merged with the measured and estimated seafloor topography grid in areas of water depth over 200 m. For the U.S. east coast, NGDC developed a nine-second grid in the area between 25°N and 50°N latitudes and 85°W and 50°W longitudes. These data were compiled from a variety of sources including:

- multibeam bathymetry surveys performed by the NOAA National Ocean Service, NOAA Ocean Exploration, USGS, and other agencies;

- hydrographic surveys data from NOAA National Ocean Service;
- bathymetric contours compiled by the Intergovernmental Oceanographic organization sponsored International Bathymetric Chart of the Caribbean Sea and the Gulf of Mexico project; and
- LIDAR data collected by the Joint Airborne LIDAR Bathymetry Technical Center of Expertise.

The vicinity of Daytona Beach is covered by a 1/3-second DEM in 28.85°N to 29.7°N latitudes and 81.4°W to 80.5°W longitudes.

### 3.3 Grid setup

In Figure 3, we present the grid extents of both reference and forecast models. Extents of C grids in both models are also shown in Figure 4. Parameters of these grids are listed in Table 1. Tsunamis hitting the Daytona Beach area will most possibly be generated along the eastern edge of the Caribbean Plate and the eastern edge of the Scotia Plate. Before they reach the Florida coasts, the waves will pass through the Bahamas, where the water is mostly shallow and the bottom topography is complex. Waves may go through complicated radiation and reflection, for which real-time simulation with nonlinear model at high resolution may be necessary. In the reference model, the A-grid covers the northern Bahamas. Shorter waves may be significantly affected by the abrupt variations of bathymetry over the continental slope. In order to capture this feature, the east boundary of A-grid is located in the deep ocean and a 20'' ( $\sim 620$  m) resolution is assigned. The B-grid is an intermediate grid, which transfers simulations from A-grid to higher-resolution C-grid. Due to shoaling effects, the long waves become shorter after entering the shallow water area over the continental shelf. Simulating these shorter waves requires higher resolution in the numerical model. In both reference and forecast models, the seaward boundaries of the B-grids are located near the edge of the continental shelf. In the reference model, the B-grid has a resolution of 5'' ( $\sim 150$  m). The reference C-grid has a resolution of 0.5'' ( $\sim 15$  m), in which the tsunami propagation and runup in the Daytona Beach area is simulated.

The reference model has very good numerical accuracy thanks to the large domain coverage and high grid resolutions. On the other hand, the reference model requires a great amount of computational resources. A 12-hour simulation in the reference model consumes a CPU time of more than 15 hours. In order to use this model for real-time forecast, the grid domains are shrunk and resolutions are downgraded in the forecast model to save CPU time. The A-, B- and C-grids in the forecast model have resolutions of 30'' ( $\sim 930$  m), 9'' ( $\sim 280$  m) and 1.5'' ( $\sim 45$  m), respectively. In a series of tests, the forecast model completes the 12-hr simulations in roughly 40 minutes of CPU time on a 2×6 core @ 2.93 GHz workstation. A tsunami originated in the nearest eastern Caribbean region may arrive at the shoreline of Daytona Beach within 4 hours. The current forecast model is capable of signaling whether a warning is required in less than an hour following the earthquake, giving the city more than 3 hours for preparation.

In a forecast model, time series of water surface elevations will be output at a reference point in C-grid during a tsunami event. These data will be employed in early stage to

predict the severity of potential tsunami impact in this area. Detailed forecast results, which include the distribution of maximum water surface elevations and flooded coastal areas, can be obtained after the model simulation is finished. If a tide gauge is operated in this area, the reference point is usually chosen at the gauge station so that the numerical model can be validated against real-time gauge measurements. In case a tide gauge does not exist, a numerical reference point can be chosen near the coast. There was a tide gauge offshore of Daytona Beach, but it has been out of operation since January 1 1980. In both reference and forecast models, we chose a numerical reference point at (29.2075°N, 80.9935°W), where the water depth is 4.81 m. The bathymetry and topography of the C-grid in the forecast model, as well as the location of the reference point, are plotted in Figure 4.

In both the forecast and reference models, simulations are initiated when the input water surface displacement exceeds a critical value of 0.001 m along the open boundaries of A-grids. The seabed friction over the wide continental shelf may dissipate a great amount of wave energy. To approximate this force, we employ a constant Manning’s roughness coefficient of 0.03 in all the grids. This value is typical for coastal waters (Bryant, 2001). On the dry land covered by vegetation, employing this Manning coefficient may underestimate the bottom friction and result in higher runup.

## 4 Model Testing

Before integration into the SIFT system, a forecast model needs to be tested for accuracy and robustness. Accuracy of the numerical model determines the reliability of the forecast. Model instability may cause the failure of the tsunami forecast in a real event and should be avoided beforehand.

### 4.1 Accuracy

Accuracy of the numerical model may be compromised by inaccurate bathymetry and topography, as well as numerical errors, such as numerical dispersion and diffusion. Numerical errors are inherent in the finite difference scheme of MOST, and are larger for coarser resolutions. The best approach to validate a forecast model is through the simulation of historical events. The Daytona Beach area has not been hit by major tsunamis in recent history. Usable data of recorded tsunami wave heights, as well as measured coastal runup and inundation, are unavailable for model validation. In this study, we investigate the effects of numerical dispersion and diffusion in the forecast model in a series of synthetic tsunami scenarios. The synthetic scenarios are simulated with both forecast and reference models. Good agreement between the two models will be observed if the accuracy of the forecast model is not compromised by the downgraded resolution. The synthetic scenarios include 6 mega tsunamis and a tsunami generated by an Mw 7.5 earthquake. The characteristics of these scenarios are presented in Table 2. Locations of the unit sources in the Atlantic basin are presented in Figs. B1 and B2, and the parameters described in Tables B1 and B2.

In Figs. 6-12, we present the simulation results of the synthetic scenarios. The time series of water surface elevations are output at the reference point from both forecast and reference models, and compared in the figures. In the scenarios of ATSZ 38-47 and ATSZ B52, the wave trains are led by several waves of shorter lengths. In this situation, the numerical

simulation becomes very sensitive to grid resolution. Although slightly larger differences are observed for these scenarios, the agreement between the forecast and reference models is still good. In all the other scenarios, the agreement is nearly perfect for the first waves. In most scenarios, the highest wave heights are seen in the leading waves.

In the scenario of ATSZ 68-77, the wave train is led by a very long wave followed by another long wave of higher wave height. The second wave arrives roughly 10 hours from the time of the earthquake. In this scenario, the second wave may also cause significant flooding in the community and should be included in the forecast simulation. The present configuration requires that the forecast simulation be run for a time period of 12 hours after the tsunami propagates into A-grid, to guarantee that all major waves are considered. In Figs. 6-12, we also compare the maximum water surface elevations predicted in both forecast and reference models. The distribution of maximum water surface elevations is consistent in the 2 models except minor differences.

The most severe tsunami flooding is observed in the synthetic scenario of ATSZ 48-57. A maximum water surface elevation of 4.05 m is observed at the warning point, where the water depth is 4.81 m. A runup of 4.75 m is present on the dry land of Daytona Beach. In reality, this wave would have already broken before it reaches the shoreline, and a great amount of energy dissipated. Wave breaking is not considered in MOST and therefore, wave height and coastal runup may be greatly overestimated in this situation.

## 4.2 Stability

A numerical model may become unstable for very large or very small input wave conditions. The six mega tsunami scenarios represent events of extremely low possibility. In recent centuries, such an event has not been observed in the Atlantic basin. For all these scenarios, there is no stability problem observed in the forecast model. The stability of the forecast model is also tested against a synthetic micro tsunami scenario, denoted as SSSZ B11. The waves input along the model boundaries are too weak to initiate the forecast model. In order to test the model for such an extremely small event, we temporarily reduce this criterion of input water surface displacement to 0.00001 m. The model performs a 12-hr simulation without any stability problems. All these tests indicate that the forecast model is quite robust and is unlikely to fail in the forecast of real tsunami events.

## 5 Conclusions

In this study, we have developed a tsunami forecast model for Daytona Beach, Florida. The model is to be integrated into the SIFT system that provides real-time forecast of tsunami arrival time, wave heights and coastal inundation for the at-risk communities of the U.S. and territories. The forecast model consists of a numerical model, which runs in 3 nested grids constructed with the best available bathymetric and topographic data sources. The innermost grid covers the population and economic center of Daytona Beach at a spatial resolution of  $\sim 45$  m. The present model is configured to run a simulation of 12 hours in a CPU time of 40 minutes on a  $2 \times 6$  core @ 2.93 GHz workstation.

Due to the lack of data, the present model is not validated against historical tsunami events. The numerical errors inherent in the lower-resolution forecast model are investigated

by comparing the forecast model to simulations with a very high resolution reference model for a series of synthetic tsunami scenarios. Comparisons of computational results between the forecast and reference models show very good agreement and indicate that the forecast model is accurate. Stability of the forecast model was also tested using synthetic scenarios.

This model is also tested in the SIFT system for four synthetic scenarios (Table C1). Computational results from the SIFT system are presented in Figs. C1-C3, and compared with those obtained in the model development in Table C2. Very good consistency is observed.

## **Acknowledgement**

This work is funded by the Joint Institute for the Study of the Atmosphere and Ocean (JISAO) under NOAA Cooperative Agreement Numbers NA10OAR4320148 and NA08OAR4320899 and is JISAO contribution number No. 2098. This work is also Contribution No. 3371 from NOAA/Pacific Marine Environmental Laboratory. The first author thanks Dr. Yong Wei for his help with Figure 5, and Dr. Aurelio Mercado Irizarry for his works on model development.

## References

- Bryant, E. (2001), *Tsunami: the Underrated Hazard*, Cambridge University Press, 320 pp.
- Churchill, D. D., Houston, S. H., and Bond, N. A. (1995), The Daytona Beach wave of 3–4 July 1992: A shallow-water gravity wave forced by a propagating squall line, *Bulletin of the American Meteorological Society*, 76(1), 21–32.
- Driscoll, N. W., Weissen, J. K., and Goff, J. A. (2000), Potential for large-scale submarine slope failure and tsunami generation along the U.S. mid-Atlantic coast, *Geology*, 20(5), 4407–4410.
- Gica, E., Spillane, M. C., Titov, V. V., Chamberlin, C. D., and Newman, J. C. (2008), Development of the forecast propagation database for NOAA's Short-Term Inundation Forecast for Tsunamis (SIFT), *NOAA Tech. Memo. OAR PMEL-139*, Pacific Marine Environmental Laboratory, NOAA, Seattle, WA, 89 pp.
- Løvholt, F., Pedersen, G., and Gisler, G. (2008), Oceanic propagation of a potential tsunami from the La Palma Island, *J. Geophys. Res.*, 113, C09026, doi:10.1029/2007JC004603.
- Percival, D. B., Arcas, D., Denbo, D. W., Eble, M. C., Gica, E., Mofjeld, H. O., Spillane, M. C., Tang, L., and Titov, V. V. (2009), Extracting tsunami source parameters via inversion of DART buoy data, *NOAA Tech. Memo. OAR PMEL-144*, Pacific Marine Environmental Laboratory, NOAA, Seattle, WA, 22 pp.
- Synolakis, C. E., Bernard, E. N., Titov, V. V., Kânoğlu, U., and González, F. I. (2008): Validation and verification of tsunami numerical models, *Pure Appl. Geophys.*, 165(11-12), 2197–2228.
- Tang, L., Titov, V. V., Wei, Y., Mofjeld, H. O., Spillane, M., Arcas, D., Bernard, E. N., Chamberlin, C. D., Gica, E., and Newman, J. (2008), Tsunami forecast analysis for the May 2006 Tonga tsunami, *J. Geophys. Res.*, 113, C12015, doi: 10.1029/2008JC004922.
- Tang L., Titov, V. V., and Chamberlin, C. D. (2009), Development, testing, and applications of site-specific tsunami inundation models for real-time forecasting, *J. Geophys. Res.*, 6, doi: 10.1029/2009JC005476.
- Ten Brink, U., Twichell, D., Geist, E., Chaytor, J., Locat, J., Lee, H., Buczkowski, B., Barkan, R., Solow, A., Andrews, B., Parsons, T., Lynett, P., Lin, J., and Sansoucy, M. (2008), Evaluation of tsunami sources with the potential to impact the U.S. Atlantic and Gulf coasts, USGS Administrative Report to the Nuclear Regulatory Commission, 300 pp.
- Titov, V. V. and González, F. I. (1997), Implementation and testing of the Method of Splitting Tsunami (MOST) model, *NOAA Tech. Memo, ERL PMEL-112*, Pacific Marine Environmental Laboratory, NOAA, Seattle, WA, 11 pp.
- Titov V. V., González F. I., Bernard E. N., Eble M. C., Mofjeld H. O., Newman J. C., Venturato A. J. (2005), Real-time tsunami forecasting: challenges and solutions, *Nat. Hazards*, 35, 41–58.

- Titov, V. V. (2009), Tsunami forecasting. In: E. N. Bernard and A. R. Robinson (edited) *The Sea*, Vol. 15, Chapter 12, Harvard University Press, Cambridge, MA, and London, U.K., 371–400.
- Wei, Y., Bernard, E. N., Tang, L., Weiss, R., Titov, V. V., Moore, C., Spillane, M., Hopkins, M., and Kânoğlu, U. (2008), Real-time experimental forecast of the Peruvian tsunami of August 2007 for U.S. coastlines, *Geophys. Res. Lett.*, *35*, L04609, doi:10.1029/2007GL032250.
- Zhou, H., Moore, C. W., Wei, Y., and Titov, V. V. (2011), A nested-grid Boussinesq-type approach to modelling dispersive propagation and runup of landslide-generated tsunamis, *Nat. Hazards Earth Syst. Sci.*, *11*(10), doi: 10.5194/nhess-11-2677-2011, 2677–2697.



Figure 1: Aerial view of Daytona Beach, Florida.

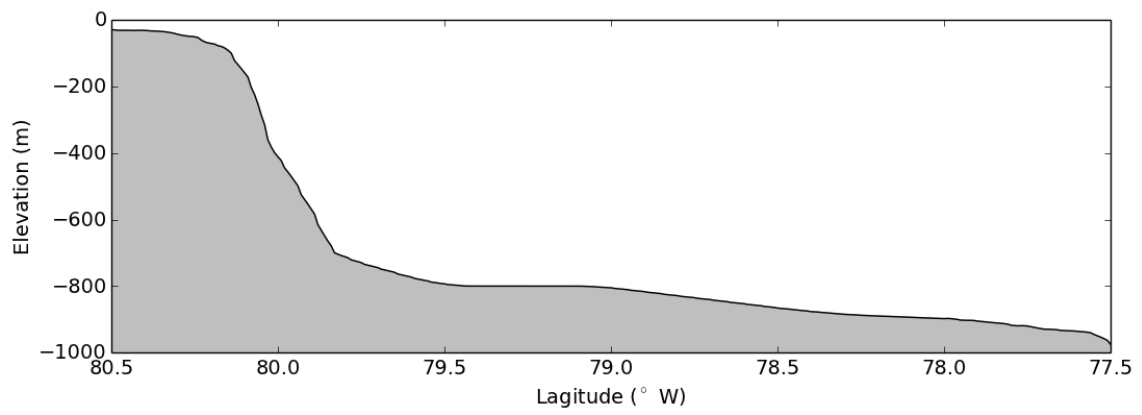


Figure 2: Transect of bathymetry along 29.2°N latitude.

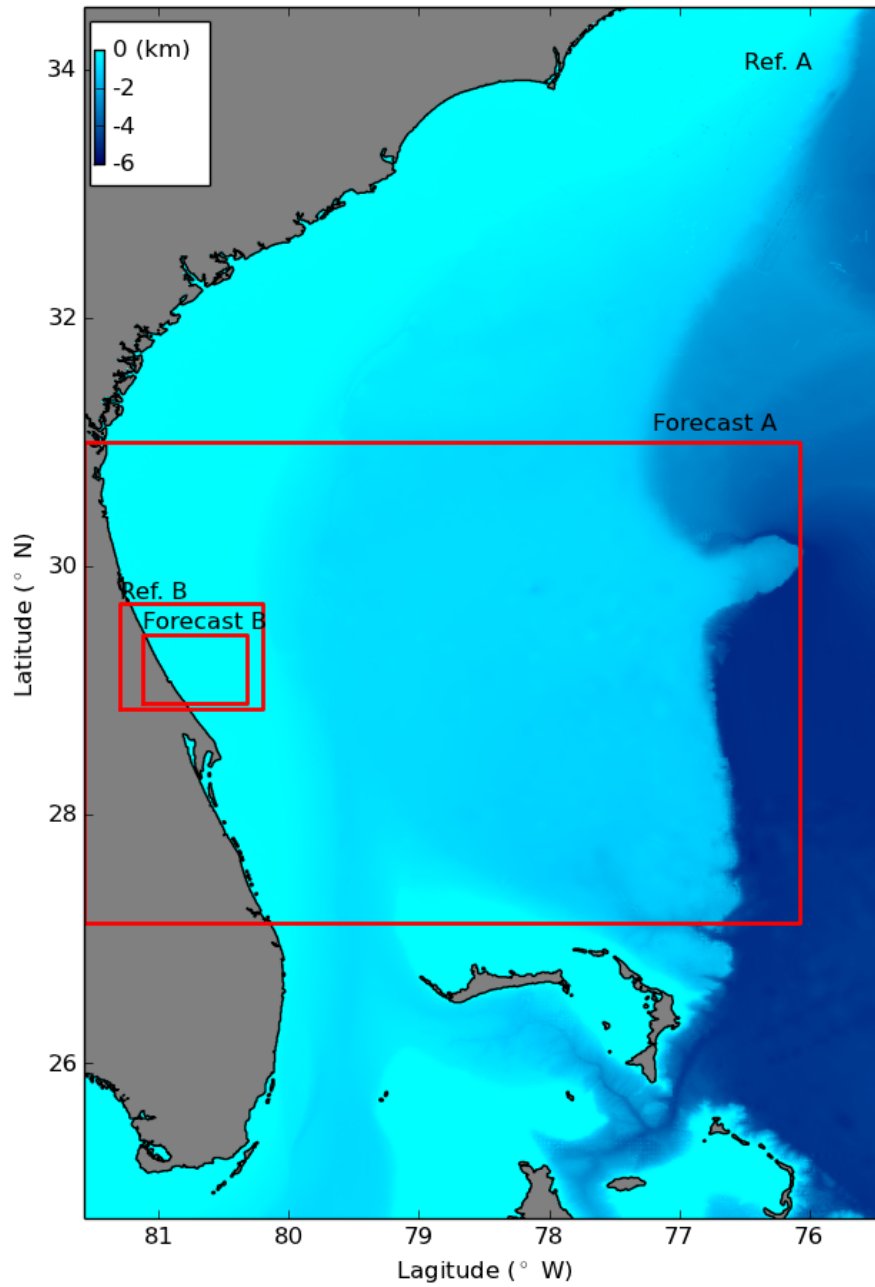


Figure 3: Extents of A- and B-grids in Daytona Beach, Florida reference and forecast models.

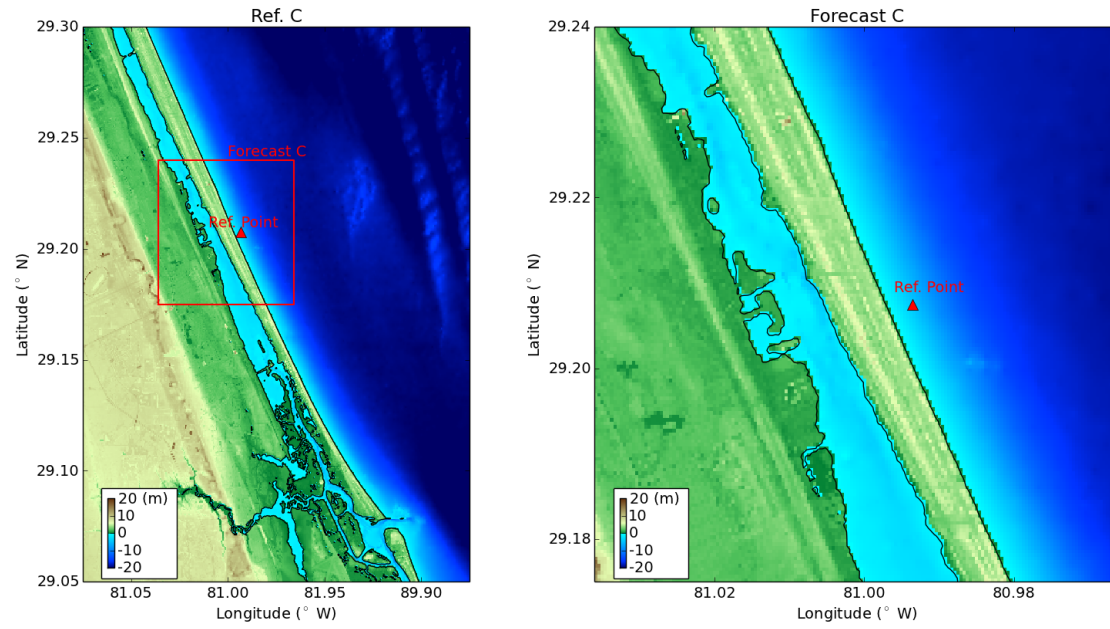


Figure 4: Topography and bathymetry of C-grids in the reference and forecast models.

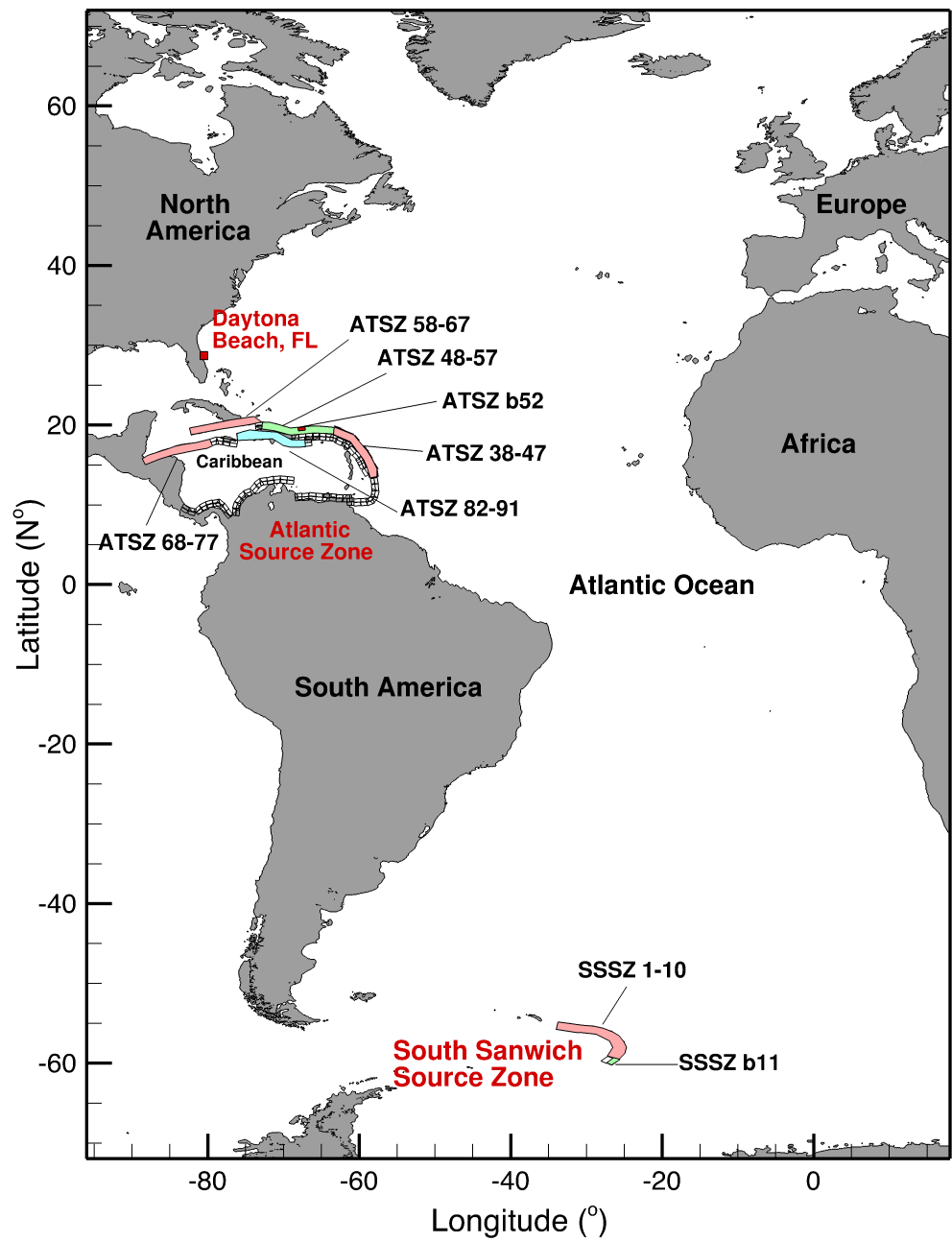


Figure 5: Map of the Atlantic Ocean showing the unit sources in synthetic tsunami scenarios.

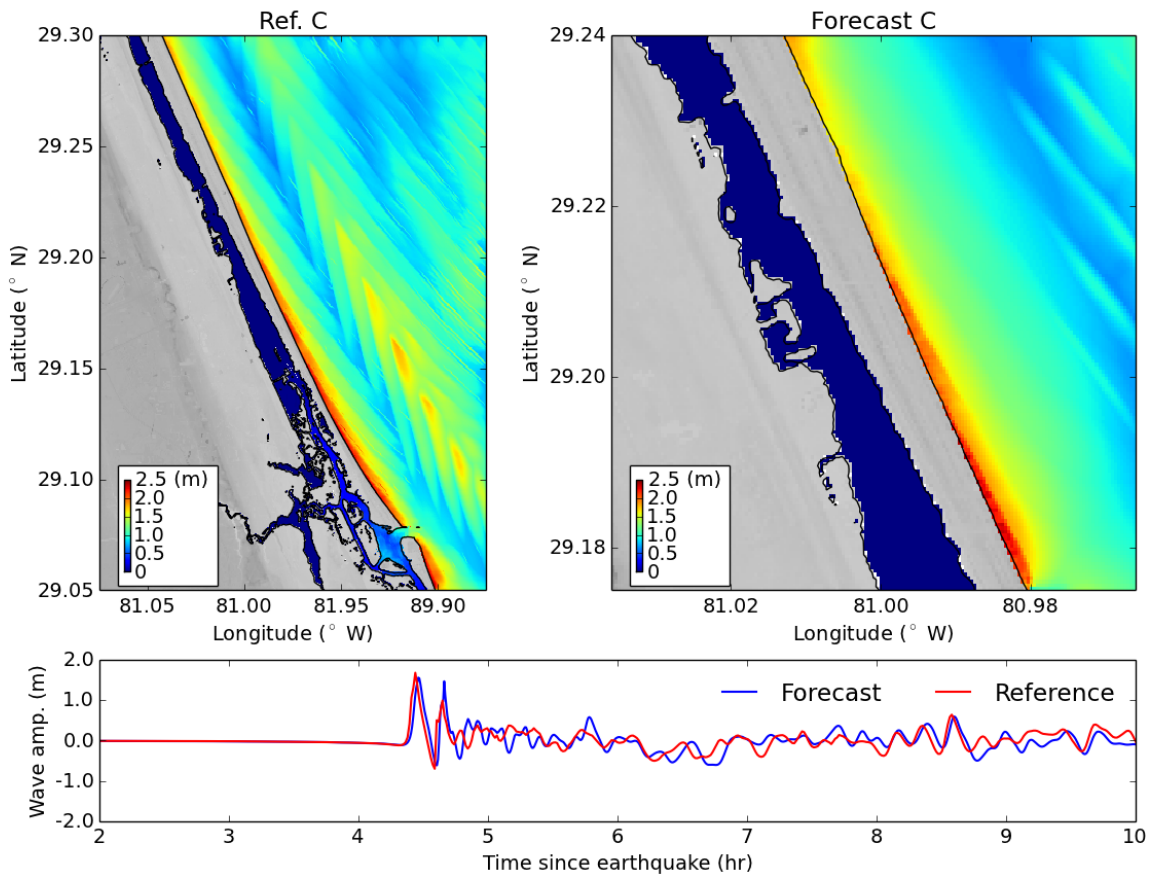


Figure 6: Model results for the synthetic scenario of ATSZ 38-47. The upper panels show the distribution of maximum water surface elevations. The lower panel shows the time series of water surface elevations at the reference point.

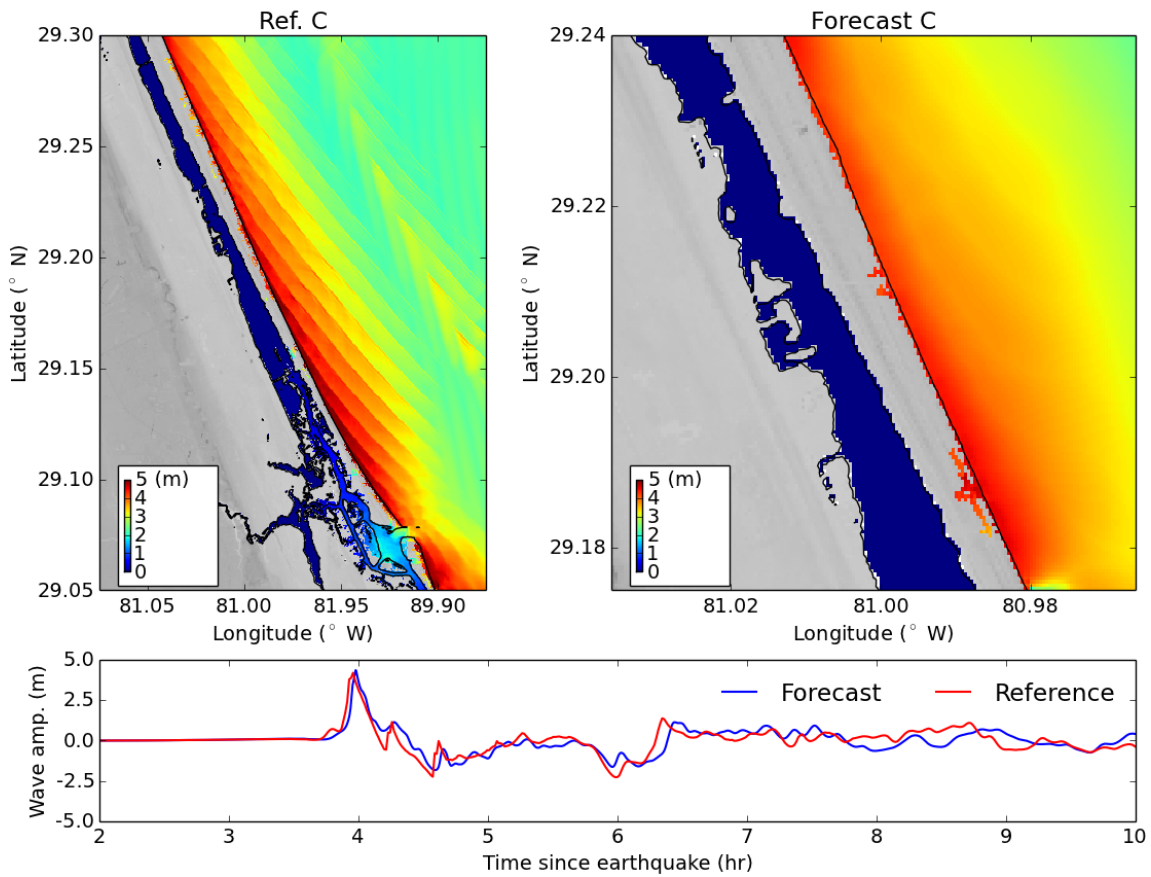


Figure 7: Model results for the synthetic scenario of ATSZ 48-57. The upper panels show the distribution of maximum water surface elevations. The lower panel shows the time series of water surface elevations at the reference point.

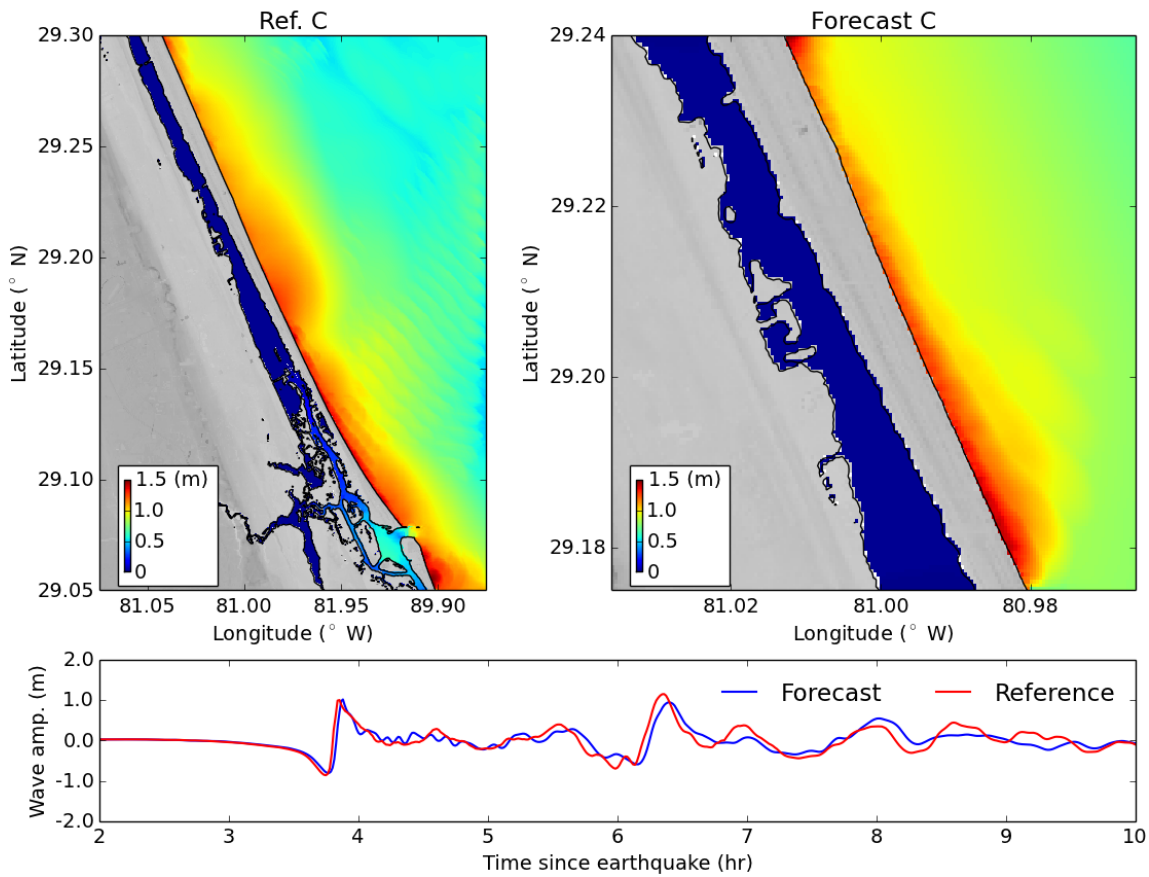


Figure 8: Model results for the synthetic scenario of ATSZ 58-67. The upper panels show the distribution of maximum water surface elevations. The lower panel shows the time series of water surface elevations at the reference point.

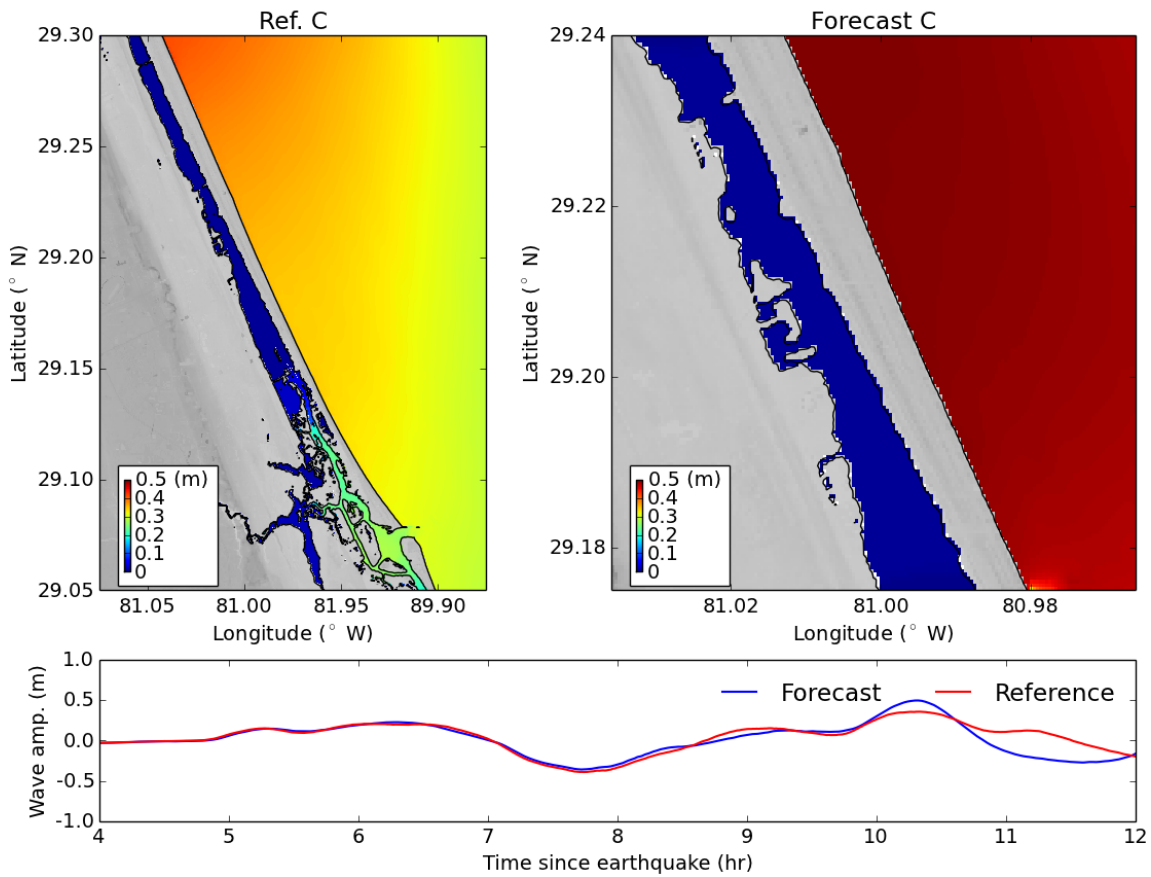


Figure 9: Model results for the synthetic scenario of ATSZ 68-77. The upper panels show the distribution of maximum water surface elevations. The lower panel shows the time series of water surface elevations at the reference point.

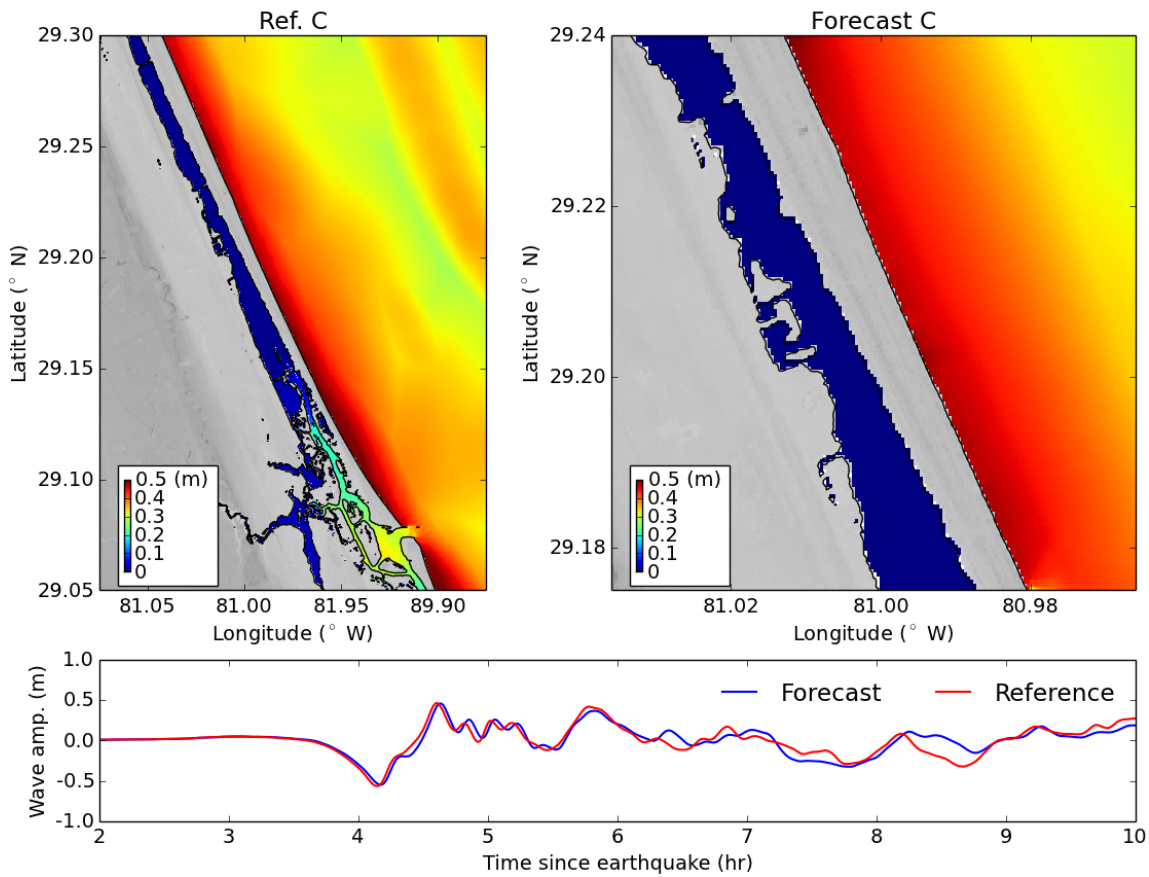


Figure 10: Model results for the synthetic scenario of ATSZ 82-91. The upper panels show the distribution of maximum water surface elevations. The lower panel shows the time series of water surface elevations at the reference point.

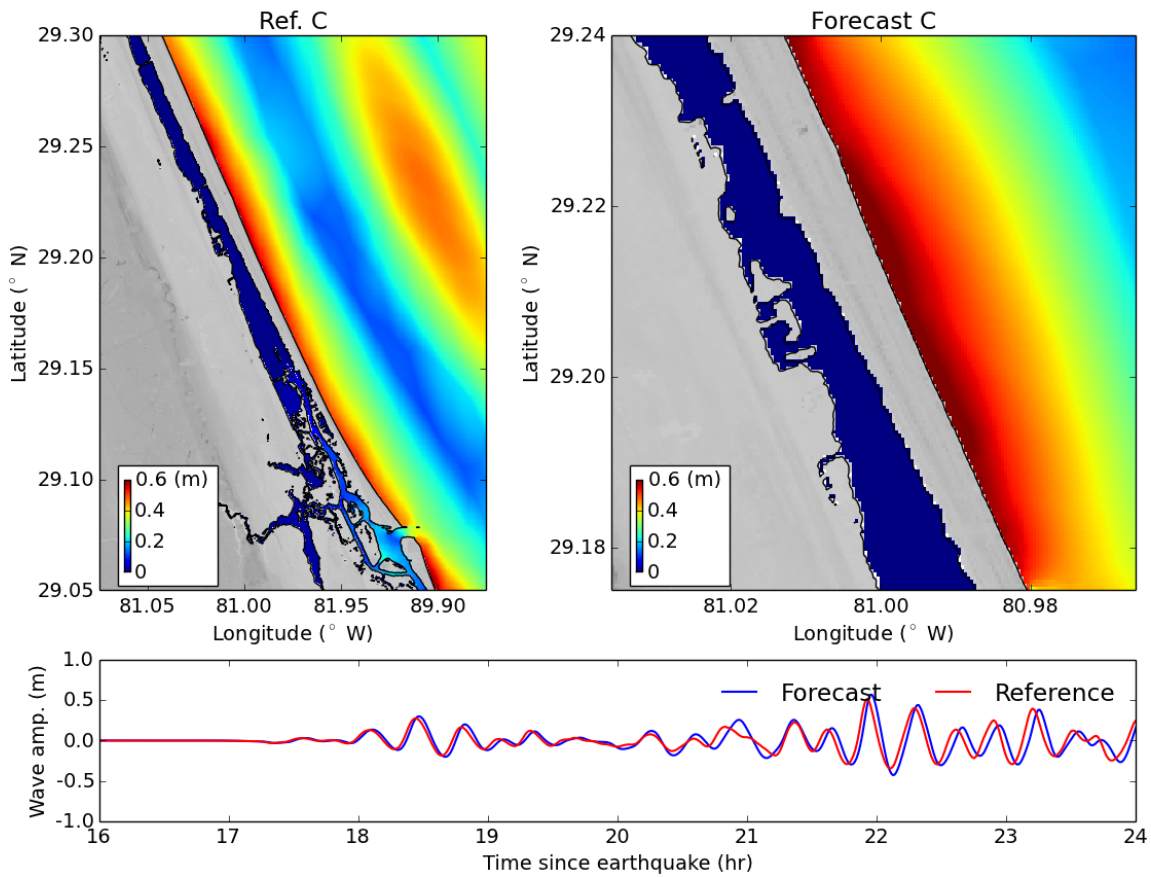


Figure 11: Model results for the synthetic scenario of SSSZ 1-10. The upper panels show the distribution of maximum water surface elevations. The lower panel shows the time series of water surface elevations at the reference point.

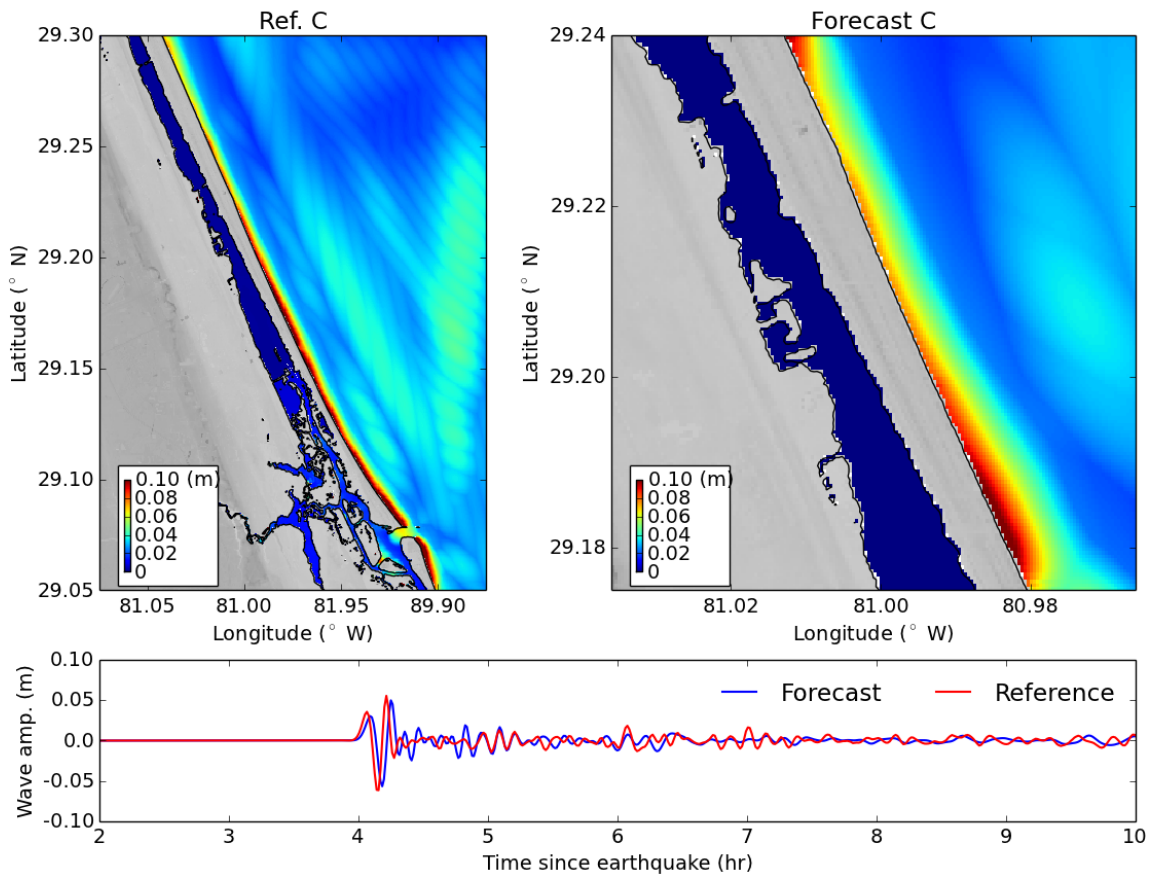


Figure 12: Model results for the synthetic scenario of ATSZ B52. The upper panels show the distribution of maximum water surface elevations. The lower panel shows the time series of water surface elevations at the reference point.

Table 1: MOST setup of the reference and forecast models for Daytona Beach, Florida.

Grid	Region	Reference Model				Forecast Model			
		Coverage Lat. ( $^{\circ}$ N) Lon. ( $^{\circ}$ W)	Cell Size	$n_x \times n_y$	Time Step (sec.)	Coverage Lat. ( $^{\circ}$ N) Lon. ( $^{\circ}$ W)	Cell Size	$n_x \times n_y$	Time Step (sec.)
A	Mid & South U.S. East Coast	24.75–34.5 81.575–75.425	20''	1108 $\times$ 1756	1.8	27.125–31.0 81.575–76.075	30''	661 $\times$ 466	2.4
B	North Florida	28.85–29.7 81.3–80.2	5''	793 $\times$ 613	1.8	28.9–29.45 81.12–80.32	9''	321 $\times$ 221	9.6
C	Daytona Beach	29.05–29.3 81.075–80.875	0.5''	1441 $\times$ 1801	0.6	29.175–29.24 81.036–80.966	1.5''	169 $\times$ 157	2.4
Minimum offshore depth (m)					1.0				
Water depth for dry land (m)					0.1				
Friction coefficient ( $n^2$ )					0.0009				
CPU time for a 12-hr simulation						~ 40 min			

Table 2: Synthetic tsunami scenarios employed to test the Daytona Beach, Florida reference and forecast models.

Scenario No.	Scenario Name	Source Zone	Tsunami Source	$\alpha$ [m]
<b>Mega-tsunami Scenario</b>				
1	ATSZ 38-47	Atlantic	A38-A47, B38-B47	25
2	ATSZ 48-57	Atlantic	A48-A57, B48-B57	25
3	ATSZ 58-67	Atlantic	A58-A67, B58-B67	25
4	ATSZ 68-77	Atlantic	A68-A77, B68-B77	25
5	ATSZ 82-91	Atlantic	A82-A91, B82-B91	25
6	SSSZ 1-10	South Sandwich	A1-A10, B1-B10	25
<b>Mw 7.5 Scenario</b>				
7	ATSZ B52	Atlantic	B52	1
<b>Micro-tsunami Scenario</b>				
8	SSSZ B11	South Sandwich	B11	0.01

## A Model \*.in files for Daytona Beach, FL

### A.1 Reference model \*.in file

0.001	Minimum amp. of input offshore wave (m)
1.0	Minimum depth of offshore (m)
0.1	Dry land depth of inundation (m)
0.0009	Friction coefficient ( $n^{**2}$ )
1	run up in a and b
300.0	max wave height meters
0.6	time step (sec)
72000	number of steps for 12 h simulation
3	Compute "A" arrays every n-th time step, n=
3	Compute "B" arrays every n-th time step, n=
90	Input number of steps between snapshots
0	...starting from
1	...saving grid every n-th node, n=

### A.2 Forecast model \*.in file

0.001	Minimum amp. of input offshore wave (m)
1.0	Minimum depth of offshore (m)
0.1	Dry land depth of inundation (m)
0.0009	Friction coefficient ( $n^{**2}$ )
1	run up in a and b
300.0	max wave height meters
2.4	time step (sec)
18000	number of steps for 12 h simulation
1	Compute "A" arrays every n-th time step, n=
4	Compute "B" arrays every n-th time step, n=
12	Input number of steps between snapshots
0	...starting from
1	...saving grid every n-th node, n=

**B Propagation Database:  
Atlantic Ocean Unit Sources**

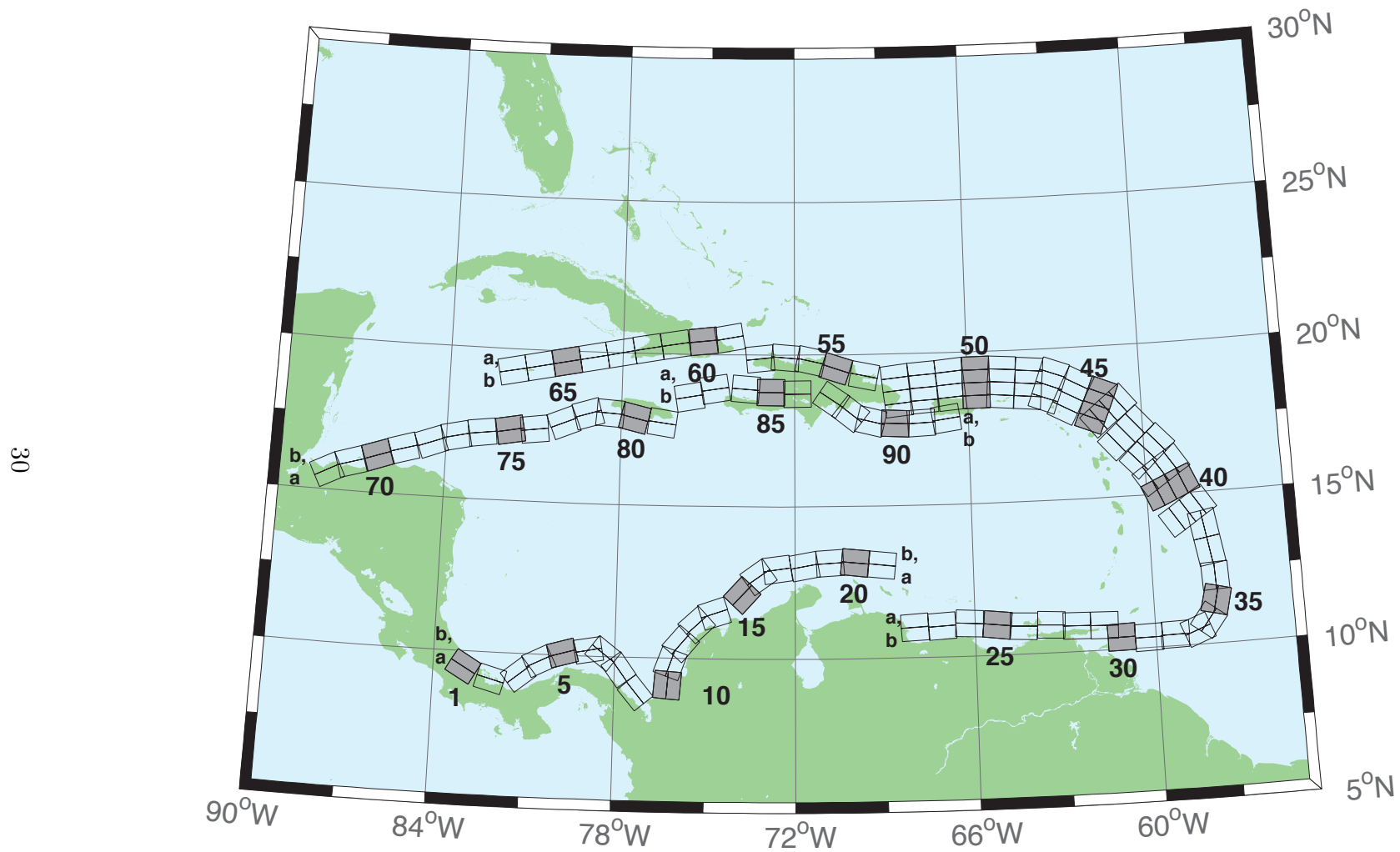


Figure B1: Atlantic Source Zone unit sources.

Table B1: Earthquake parameters for Atlantic Source Zone unit sources.

Segment	Description	Longitude(°E)	Latitude(°N)	Strike(°)	Dip(°)	Depth (km)
atsz-1a	Atlantic Source Zone	-83.2020	9.1449	120	27.5	28.09
atsz-1b	Atlantic Source Zone	-83.0000	9.4899	120	27.5	5
atsz-2a	Atlantic Source Zone	-82.1932	8.7408	105.1	27.5	28.09
atsz-2b	Atlantic Source Zone	-82.0880	9.1254	105.1	27.5	5
atsz-3a	Atlantic Source Zone	-80.9172	9.0103	51.31	30	30
atsz-3b	Atlantic Source Zone	-81.1636	9.3139	51.31	30	5
atsz-4a	Atlantic Source Zone	-80.3265	9.4308	63.49	30	30
atsz-4b	Atlantic Source Zone	-80.5027	9.7789	63.49	30	5
atsz-5a	Atlantic Source Zone	-79.6247	9.6961	74.44	30	30
atsz-5b	Atlantic Source Zone	-79.7307	10.0708	74.44	30	5
atsz-6a	Atlantic Source Zone	-78.8069	9.8083	79.71	30	30
atsz-6b	Atlantic Source Zone	-78.8775	10.1910	79.71	30	5
atsz-7a	Atlantic Source Zone	-78.6237	9.7963	127.2	30	30
atsz-7b	Atlantic Source Zone	-78.3845	10.1059	127.2	30	5
atsz-8a	Atlantic Source Zone	-78.1693	9.3544	143.8	30	30
atsz-8b	Atlantic Source Zone	-77.8511	9.5844	143.8	30	5
atsz-9a	Atlantic Source Zone	-77.5913	8.5989	139.9	30	30
atsz-9b	Atlantic Source Zone	-77.2900	8.8493	139.9	30	5
atsz-10a	Atlantic Source Zone	-75.8109	9.0881	4.67	17	19.62
atsz-10b	Atlantic Source Zone	-76.2445	9.1231	4.67	17	5
atsz-11a	Atlantic Source Zone	-75.7406	9.6929	19.67	17	19.62
atsz-11b	Atlantic Source Zone	-76.1511	9.8375	19.67	17	5
atsz-12a	Atlantic Source Zone	-75.4763	10.2042	40.4	17	19.62
atsz-12b	Atlantic Source Zone	-75.8089	10.4826	40.4	17	5
atsz-13a	Atlantic Source Zone	-74.9914	10.7914	47.17	17	19.62
atsz-13b	Atlantic Source Zone	-75.2890	11.1064	47.17	17	5
atsz-14a	Atlantic Source Zone	-74.5666	11.0708	71.68	17	19.62
atsz-14b	Atlantic Source Zone	-74.7043	11.4786	71.68	17	5
atsz-15a	Atlantic Source Zone	-73.4576	11.8012	42.69	17	19.62
atsz-15b	Atlantic Source Zone	-73.7805	12.0924	42.69	17	5
atsz-16a	Atlantic Source Zone	-72.9788	12.3365	54.75	17	19.62
atsz-16b	Atlantic Source Zone	-73.2329	12.6873	54.75	17	5
atsz-17a	Atlantic Source Zone	-72.5454	12.5061	81.96	17	19.62
atsz-17b	Atlantic Source Zone	-72.6071	12.9314	81.96	17	5
atsz-18a	Atlantic Source Zone	-71.6045	12.6174	79.63	17	19.62
atsz-18b	Atlantic Source Zone	-71.6839	13.0399	79.63	17	5
atsz-19a	Atlantic Source Zone	-70.7970	12.7078	86.32	17	19.62
atsz-19b	Atlantic Source Zone	-70.8253	13.1364	86.32	17	5
atsz-20a	Atlantic Source Zone	-70.0246	12.7185	95.94	17	19.62
atsz-20b	Atlantic Source Zone	-69.9789	13.1457	95.94	17	5
atsz-21a	Atlantic Source Zone	-69.1244	12.6320	95.94	17	19.62
atsz-21b	Atlantic Source Zone	-69.0788	13.0592	95.94	17	5
atsz-22a	Atlantic Source Zone	-68.0338	11.4286	266.9	15	17.94
atsz-22b	Atlantic Source Zone	-68.0102	10.9954	266.9	15	5
atsz-23a	Atlantic Source Zone	-67.1246	11.4487	266.9	15	17.94
atsz-23b	Atlantic Source Zone	-67.1010	11.0155	266.9	15	5
atsz-24a	Atlantic Source Zone	-66.1656	11.5055	273.3	15	17.94
atsz-24b	Atlantic Source Zone	-66.1911	11.0724	273.3	15	5
atsz-25a	Atlantic Source Zone	-65.2126	11.4246	276.4	15	17.94
atsz-25b	Atlantic Source Zone	-65.2616	10.9934	276.4	15	5
atsz-26a	Atlantic Source Zone	-64.3641	11.3516	272.9	15	17.94
atsz-26b	Atlantic Source Zone	-64.3862	10.9183	272.9	15	5
atsz-27a	Atlantic Source Zone	-63.4472	11.3516	272.9	15	17.94
atsz-27b	Atlantic Source Zone	-63.4698	10.9183	272.9	15	5
atsz-28a	Atlantic Source Zone	-62.6104	11.2831	271.1	15	17.94
atsz-28b	Atlantic Source Zone	-62.6189	10.8493	271.1	15	5
atsz-29a	Atlantic Source Zone	-61.6826	11.2518	271.6	15	17.94
atsz-29b	Atlantic Source Zone	-61.6947	10.8181	271.6	15	5
atsz-30a	Atlantic Source Zone	-61.1569	10.8303	269	15	17.94
atsz-30b	Atlantic Source Zone	-61.1493	10.3965	269	15	5
atsz-31a	Atlantic Source Zone	-60.2529	10.7739	269	15	17.94
atsz-31b	Atlantic Source Zone	-60.2453	10.3401	269	15	5
atsz-32a	Atlantic Source Zone	-59.3510	10.8123	269	15	17.94

Continued on next page

Table B1 – continued from previous page

Segment	Description	Longitude(°E)	Latitude(°N)	Strike(°)	Dip(°)	Depth (km)
atsz-32b	Atlantic Source Zone	-59.3734	10.3785	269	15	5
atsz-33a	Atlantic Source Zone	-58.7592	10.8785	248.6	15	17.94
atsz-33b	Atlantic Source Zone	-58.5984	10.4745	248.6	15	5
atsz-34a	Atlantic Source Zone	-58.5699	11.0330	217.2	15	17.94
atsz-34b	Atlantic Source Zone	-58.2179	10.7710	217.2	15	5
atsz-35a	Atlantic Source Zone	-58.3549	11.5300	193.7	15	17.94
atsz-35b	Atlantic Source Zone	-57.9248	11.4274	193.7	15	5
atsz-36a	Atlantic Source Zone	-58.3432	12.1858	177.7	15	17.94
atsz-36b	Atlantic Source Zone	-57.8997	12.2036	177.7	15	5
atsz-37a	Atlantic Source Zone	-58.4490	12.9725	170.7	15	17.94
atsz-37b	Atlantic Source Zone	-58.0095	13.0424	170.7	15	5
atsz-38a	Atlantic Source Zone	-58.6079	13.8503	170.2	15	17.94
atsz-38b	Atlantic Source Zone	-58.1674	13.9240	170.2	15	5
atsz-39a	Atlantic Source Zone	-58.6667	14.3915	146.8	15	17.94
atsz-39b	Atlantic Source Zone	-58.2913	14.6287	146.8	15	5
atsz-39y	Atlantic Source Zone	-59.4168	13.9171	146.8	15	43.82
atsz-39z	Atlantic Source Zone	-59.0415	14.1543	146.8	15	30.88
atsz-40a	Atlantic Source Zone	-59.1899	15.2143	156.2	15	17.94
atsz-40b	Atlantic Source Zone	-58.7781	15.3892	156.2	15	5
atsz-40y	Atlantic Source Zone	-60.0131	14.8646	156.2	15	43.82
atsz-40z	Atlantic Source Zone	-59.6012	15.0395	156.2	15	30.88
atsz-41a	Atlantic Source Zone	-59.4723	15.7987	146.3	15	17.94
atsz-41b	Atlantic Source Zone	-59.0966	16.0392	146.3	15	5
atsz-41y	Atlantic Source Zone	-60.2229	15.3177	146.3	15	43.82
atsz-41z	Atlantic Source Zone	-59.8473	15.5582	146.3	15	30.88
atsz-42a	Atlantic Source Zone	-59.9029	16.4535	137	15	17.94
atsz-42b	Atlantic Source Zone	-59.5716	16.7494	137	15	5
atsz-42y	Atlantic Source Zone	-60.5645	15.8616	137	15	43.82
atsz-42z	Atlantic Source Zone	-60.2334	16.1575	137	15	30.88
atsz-43a	Atlantic Source Zone	-60.5996	17.0903	138.7	15	17.94
atsz-43b	Atlantic Source Zone	-60.2580	17.3766	138.7	15	5
atsz-43y	Atlantic Source Zone	-61.2818	16.5177	138.7	15	43.82
atsz-43z	Atlantic Source Zone	-60.9404	16.8040	138.7	15	30.88
atsz-44a	Atlantic Source Zone	-61.1559	17.8560	141.1	15	17.94
atsz-44b	Atlantic Source Zone	-60.8008	18.1286	141.1	15	5
atsz-44y	Atlantic Source Zone	-61.8651	17.3108	141.1	15	43.82
atsz-44z	Atlantic Source Zone	-61.5102	17.5834	141.1	15	30.88
atsz-45a	Atlantic Source Zone	-61.5491	18.0566	112.8	15	17.94
atsz-45b	Atlantic Source Zone	-61.3716	18.4564	112.8	15	5
atsz-45y	Atlantic Source Zone	-61.9037	17.2569	112.8	15	43.82
atsz-45z	Atlantic Source Zone	-61.7260	17.6567	112.8	15	30.88
atsz-46a	Atlantic Source Zone	-62.4217	18.4149	117.9	15	17.94
atsz-46b	Atlantic Source Zone	-62.2075	18.7985	117.9	15	5
atsz-46y	Atlantic Source Zone	-62.8493	17.6477	117.9	15	43.82
atsz-46z	Atlantic Source Zone	-62.6352	18.0313	117.9	15	30.88
atsz-47a	Atlantic Source Zone	-63.1649	18.7844	110.5	20	22.1
atsz-47b	Atlantic Source Zone	-63.0087	19.1798	110.5	20	5
atsz-47y	Atlantic Source Zone	-63.4770	17.9936	110.5	20	56.3
atsz-47z	Atlantic Source Zone	-63.3205	18.3890	110.5	20	39.2
atsz-48a	Atlantic Source Zone	-63.8800	18.8870	95.37	20	22.1
atsz-48b	Atlantic Source Zone	-63.8382	19.3072	95.37	20	5
atsz-48y	Atlantic Source Zone	-63.9643	18.0465	95.37	20	56.3
atsz-48z	Atlantic Source Zone	-63.9216	18.4667	95.37	20	39.2
atsz-49a	Atlantic Source Zone	-64.8153	18.9650	94.34	20	22.1
atsz-49b	Atlantic Source Zone	-64.7814	19.3859	94.34	20	5
atsz-49y	Atlantic Source Zone	-64.8840	18.1233	94.34	20	56.3
atsz-49z	Atlantic Source Zone	-64.8492	18.5442	94.34	20	39.2
atsz-50a	Atlantic Source Zone	-65.6921	18.9848	89.59	20	22.1
atsz-50b	Atlantic Source Zone	-65.6953	19.4069	89.59	20	5
atsz-50y	Atlantic Source Zone	-65.6874	18.1407	89.59	20	56.3
atsz-50z	Atlantic Source Zone	-65.6887	18.5628	89.59	20	39.2
atsz-51a	Atlantic Source Zone	-66.5742	18.9484	84.98	20	22.1
atsz-51b	Atlantic Source Zone	-66.6133	19.3688	84.98	20	5
atsz-51y	Atlantic Source Zone	-66.4977	18.1076	84.98	20	56.3

Continued on next page

Table B1 – continued from previous page

Segment	Description	Longitude(°E)	Latitude(°N)	Strike(°)	Dip(°)	Depth (km)
atsz-51z	Atlantic Source Zone	-66.5353	18.5280	84.98	20	39.2
atsz-52a	Atlantic Source Zone	-67.5412	18.8738	85.87	20	22.1
atsz-52b	Atlantic Source Zone	-67.5734	19.2948	85.87	20	5
atsz-52y	Atlantic Source Zone	-67.4781	18.0319	85.87	20	56.3
atsz-52z	Atlantic Source Zone	-67.5090	18.4529	85.87	20	39.2
atsz-53a	Atlantic Source Zone	-68.4547	18.7853	83.64	20	22.1
atsz-53b	Atlantic Source Zone	-68.5042	19.2048	83.64	20	5
atsz-53y	Atlantic Source Zone	-68.3575	17.9463	83.64	20	56.3
atsz-53z	Atlantic Source Zone	-68.4055	18.3658	83.64	20	39.2
atsz-54a	Atlantic Source Zone	-69.6740	18.8841	101.5	20	22.1
atsz-54b	Atlantic Source Zone	-69.5846	19.2976	101.5	20	5
atsz-55a	Atlantic Source Zone	-70.7045	19.1376	108.2	20	22.1
atsz-55b	Atlantic Source Zone	-70.5647	19.5386	108.2	20	5
atsz-56a	Atlantic Source Zone	-71.5368	19.3853	102.6	20	22.1
atsz-56b	Atlantic Source Zone	-71.4386	19.7971	102.6	20	5
atsz-57a	Atlantic Source Zone	-72.3535	19.4838	94.2	20	22.1
atsz-57b	Atlantic Source Zone	-72.3206	19.9047	94.2	20	5
atsz-58a	Atlantic Source Zone	-73.1580	19.4498	84.34	20	22.1
atsz-58b	Atlantic Source Zone	-73.2022	19.8698	84.34	20	5
atsz-59a	Atlantic Source Zone	-74.3567	20.9620	259.7	20	22.1
atsz-59b	Atlantic Source Zone	-74.2764	20.5467	259.7	20	5
atsz-60a	Atlantic Source Zone	-75.2386	20.8622	264.2	15	17.94
atsz-60b	Atlantic Source Zone	-75.1917	20.4306	264.2	15	5
atsz-61a	Atlantic Source Zone	-76.2383	20.7425	260.7	15	17.94
atsz-61b	Atlantic Source Zone	-76.1635	20.3144	260.7	15	5
atsz-62a	Atlantic Source Zone	-77.2021	20.5910	259.9	15	17.94
atsz-62b	Atlantic Source Zone	-77.1214	20.1638	259.9	15	5
atsz-63a	Atlantic Source Zone	-78.1540	20.4189	259	15	17.94
atsz-63b	Atlantic Source Zone	-78.0661	19.9930	259	15	5
atsz-64a	Atlantic Source Zone	-79.0959	20.2498	259.2	15	17.94
atsz-64b	Atlantic Source Zone	-79.0098	19.8236	259.2	15	5
atsz-65a	Atlantic Source Zone	-80.0393	20.0773	258.9	15	17.94
atsz-65b	Atlantic Source Zone	-79.9502	19.6516	258.9	15	5
atsz-66a	Atlantic Source Zone	-80.9675	19.8993	258.6	15	17.94
atsz-66b	Atlantic Source Zone	-80.8766	19.4740	258.6	15	5
atsz-67a	Atlantic Source Zone	-81.9065	19.7214	258.5	15	17.94
atsz-67b	Atlantic Source Zone	-81.8149	19.2962	258.5	15	5
atsz-68a	Atlantic Source Zone	-87.8003	15.2509	62.69	15	17.94
atsz-68b	Atlantic Source Zone	-88.0070	15.6364	62.69	15	5
atsz-69a	Atlantic Source Zone	-87.0824	15.5331	72.73	15	17.94
atsz-69b	Atlantic Source Zone	-87.2163	15.9474	72.73	15	5
atsz-70a	Atlantic Source Zone	-86.1622	15.8274	70.64	15	17.94
atsz-70b	Atlantic Source Zone	-86.3120	16.2367	70.64	15	5
atsz-71a	Atlantic Source Zone	-85.3117	16.1052	73.7	15	17.94
atsz-71b	Atlantic Source Zone	-85.4387	16.5216	73.7	15	5
atsz-72a	Atlantic Source Zone	-84.3470	16.3820	69.66	15	17.94
atsz-72b	Atlantic Source Zone	-84.5045	16.7888	69.66	15	5
atsz-73a	Atlantic Source Zone	-83.5657	16.6196	77.36	15	17.94
atsz-73b	Atlantic Source Zone	-83.6650	17.0429	77.36	15	5
atsz-74a	Atlantic Source Zone	-82.7104	16.7695	82.35	15	17.94
atsz-74b	Atlantic Source Zone	-82.7709	17.1995	82.35	15	5
atsz-75a	Atlantic Source Zone	-81.7297	16.9003	79.86	15	17.94
atsz-75b	Atlantic Source Zone	-81.8097	17.3274	79.86	15	5
atsz-76a	Atlantic Source Zone	-80.9196	16.9495	82.95	15	17.94
atsz-76b	Atlantic Source Zone	-80.9754	17.3801	82.95	15	5
atsz-77a	Atlantic Source Zone	-79.8086	17.2357	67.95	15	17.94
atsz-77b	Atlantic Source Zone	-79.9795	17.6378	67.95	15	5
atsz-78a	Atlantic Source Zone	-79.0245	17.5415	73.61	15	17.94
atsz-78b	Atlantic Source Zone	-79.1532	17.9577	73.61	15	5
atsz-79a	Atlantic Source Zone	-78.4122	17.5689	94.07	15	17.94
atsz-79b	Atlantic Source Zone	-78.3798	18.0017	94.07	15	5
atsz-80a	Atlantic Source Zone	-77.6403	17.4391	103.3	15	17.94
atsz-80b	Atlantic Source Zone	-77.5352	17.8613	103.3	15	5
atsz-81a	Atlantic Source Zone	-76.6376	17.2984	98.21	15	17.94

Continued on next page

**Table B1 – continued from previous page**

Segment	Description	Longitude(°E)	Latitude(°N)	Strike(°)	Dip(°)	Depth (km)
atsz-81b	Atlantic Source Zone	-76.5726	17.7278	98.21	15	5
atsz-82a	Atlantic Source Zone	-75.7299	19.0217	260.1	15	17.94
atsz-82b	Atlantic Source Zone	-75.6516	18.5942	260.1	15	5
atsz-83a	Atlantic Source Zone	-74.8351	19.2911	260.8	15	17.94
atsz-83b	Atlantic Source Zone	-74.7621	18.8628	260.8	15	5
atsz-84a	Atlantic Source Zone	-73.6639	19.2991	274.8	15	17.94
atsz-84b	Atlantic Source Zone	-73.7026	18.8668	274.8	15	5
atsz-85a	Atlantic Source Zone	-72.8198	19.2019	270.6	15	17.94
atsz-85b	Atlantic Source Zone	-72.8246	18.7681	270.6	15	5
atsz-86a	Atlantic Source Zone	-71.9143	19.1477	269.1	15	17.94
atsz-86b	Atlantic Source Zone	-71.9068	18.7139	269.1	15	5
atsz-87a	Atlantic Source Zone	-70.4738	18.8821	304.5	15	17.94
atsz-87b	Atlantic Source Zone	-70.7329	18.5245	304.5	15	5
atsz-88a	Atlantic Source Zone	-69.7710	18.3902	308.9	15	17.94
atsz-88b	Atlantic Source Zone	-70.0547	18.0504	308.4	15	5
atsz-89a	Atlantic Source Zone	-69.2635	18.2099	283.9	15	17.94
atsz-89b	Atlantic Source Zone	-69.3728	17.7887	283.9	15	5
atsz-90a	Atlantic Source Zone	-68.5059	18.1443	272.9	15	17.94
atsz-90b	Atlantic Source Zone	-68.5284	17.7110	272.9	15	5
atsz-91a	Atlantic Source Zone	-67.6428	18.1438	267.8	15	17.94
atsz-91b	Atlantic Source Zone	-67.6256	17.7103	267.8	15	5
atsz-92a	Atlantic Source Zone	-66.8261	18.2536	262	15	17.94
atsz-92b	Atlantic Source Zone	-66.7627	17.8240	262	15	5

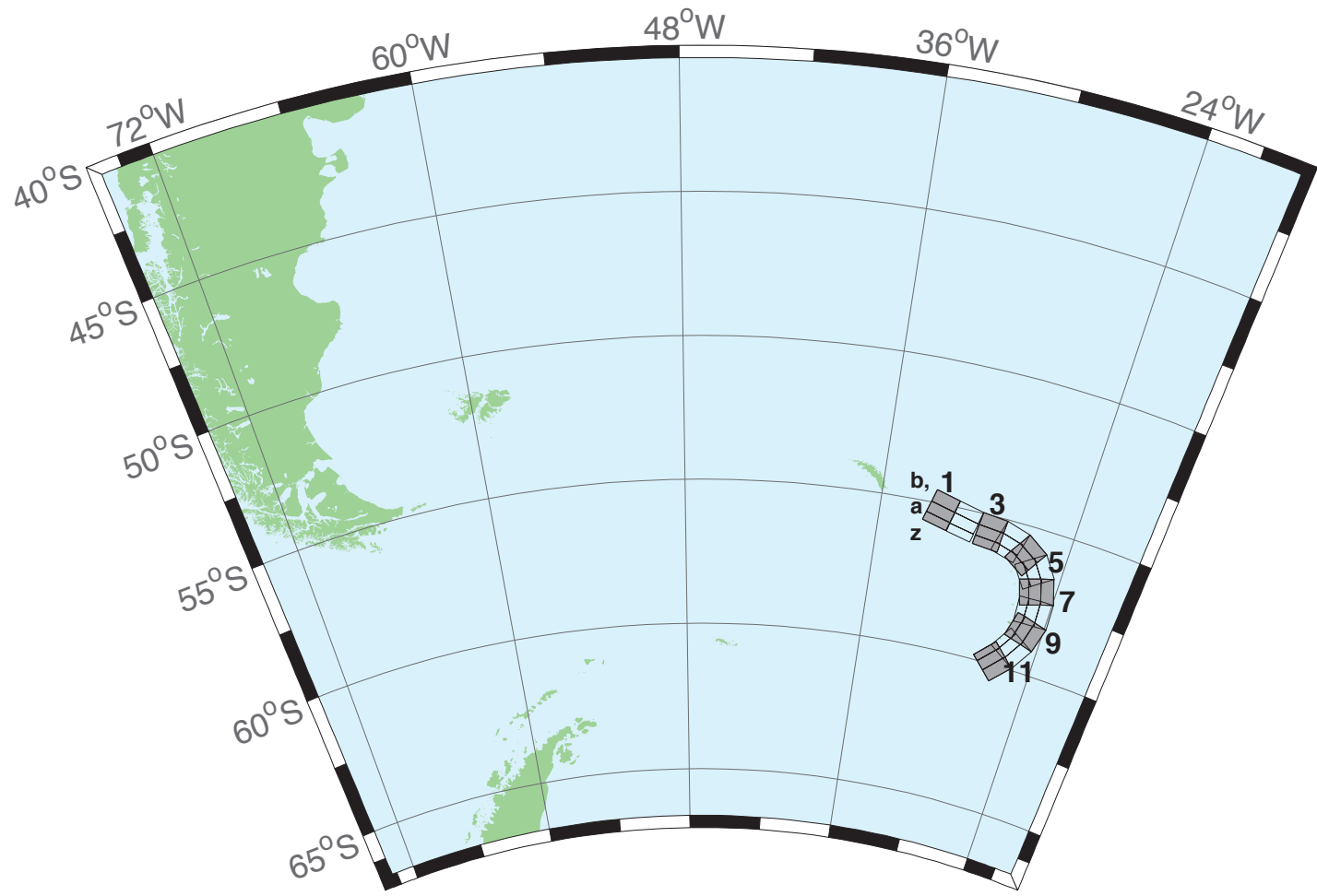


Figure B2: South Sandwich Islands Subduction Zone.

Table B2: Earthquake parameters for South Sandwich Islands Subduction Zone unit sources.

Segment	Description	Longitude(°E)	Latitude(°N)	Strike(°)	Dip(°)	Depth (km)
sssz-1a	South Sandwich Islands Subduction Zone	-32.3713	-55.4655	104.7	28.53	17.51
sssz-1b	South Sandwich Islands Subduction Zone	-32.1953	-55.0832	104.7	9.957	8.866
sssz-1z	South Sandwich Islands Subduction Zone	-32.5091	-55.7624	104.7	46.99	41.39
sssz-2a	South Sandwich Islands Subduction Zone	-30.8028	-55.6842	102.4	28.53	17.51
sssz-2b	South Sandwich Islands Subduction Zone	-30.6524	-55.2982	102.4	9.957	8.866
sssz-2z	South Sandwich Islands Subduction Zone	-30.9206	-55.9839	102.4	46.99	41.39
sssz-3a	South Sandwich Islands Subduction Zone	-29.0824	-55.8403	95.53	28.53	17.51
sssz-3b	South Sandwich Islands Subduction Zone	-29.0149	-55.4468	95.53	9.957	8.866
sssz-3z	South Sandwich Islands Subduction Zone	-29.1353	-56.1458	95.53	46.99	41.39
sssz-4a	South Sandwich Islands Subduction Zone	-27.8128	-55.9796	106.1	28.53	17.51
sssz-4b	South Sandwich Islands Subduction Zone	-27.6174	-55.5999	106.1	9.957	8.866
sssz-4z	South Sandwich Islands Subduction Zone	-27.9659	-56.2744	106.1	46.99	41.39
sssz-5a	South Sandwich Islands Subduction Zone	-26.7928	-56.2481	123.1	28.53	17.51
sssz-5b	South Sandwich Islands Subduction Zone	-26.4059	-55.9170	123.1	9.957	8.866
sssz-5z	South Sandwich Islands Subduction Zone	-27.0955	-56.5052	123.1	46.99	41.39
sssz-6a	South Sandwich Islands Subduction Zone	-26.1317	-56.6466	145.6	23.28	16.11
sssz-6b	South Sandwich Islands Subduction Zone	-25.5131	-56.4133	145.6	9.09	8.228
sssz-6z	South Sandwich Islands Subduction Zone	-26.5920	-56.8194	145.6	47.15	35.87
sssz-7a	South Sandwich Islands Subduction Zone	-25.6787	-57.2162	162.9	21.21	14.23
sssz-7b	South Sandwich Islands Subduction Zone	-24.9394	-57.0932	162.9	7.596	7.626
sssz-7z	South Sandwich Islands Subduction Zone	-26.2493	-57.3109	162.9	44.16	32.32
sssz-8a	South Sandwich Islands Subduction Zone	-25.5161	-57.8712	178.2	20.33	15.91
sssz-8b	South Sandwich Islands Subduction Zone	-24.7233	-57.8580	178.2	8.449	8.562
sssz-8z	South Sandwich Islands Subduction Zone	-26.1280	-57.8813	178.2	43.65	33.28
sssz-9a	South Sandwich Islands Subduction Zone	-25.6657	-58.5053	195.4	25.76	15.71
sssz-9b	South Sandwich Islands Subduction Zone	-24.9168	-58.6127	195.4	8.254	8.537
sssz-9z	South Sandwich Islands Subduction Zone	-26.1799	-58.4313	195.4	51.69	37.44
sssz-10a	South Sandwich Islands Subduction Zone	-26.1563	-59.1048	212.5	32.82	15.65
sssz-10b	South Sandwich Islands Subduction Zone	-25.5335	-59.3080	212.5	10.45	6.581
sssz-10z	South Sandwich Islands Subduction Zone	-26.5817	-58.9653	212.5	54.77	42.75
sssz-11a	South Sandwich Islands Subduction Zone	-27.0794	-59.6799	224.2	33.67	15.75
sssz-11b	South Sandwich Islands Subduction Zone	-26.5460	-59.9412	224.2	11.32	5.927
sssz-11z	South Sandwich Islands Subduction Zone	-27.4245	-59.5098	224.2	57.19	43.46

## C Forecast Model Testing

Authors: Nazila Merati, Yong Wei, and Jean Newman

### C.1 Purpose

Forecast models are tested with synthetic tsunami events covering a range of tsunami source locations. Testing is also done with selected historical tsunami events when available.

The purpose of forecast model testing is three-fold. The first objective is to assure that the results obtained with NOAA's tsunami forecast system, which has been released to the Tsunami Warning Centers for operational use, are identical to those obtained by the researcher during the development of the forecast model. The second objective is to test the forecast model for consistency, accuracy, time efficiency, and quality of results over a range of possible tsunami locations and magnitudes. The third objective is to identify bugs and issues in need of resolution by the researcher who developed the Forecast Model or by the forecast software development team before the next version release to NOAA's two Tsunami Warning Centers.

Local hardware and software applications, and tools familiar to the researcher(s), are used to run the Method of Splitting Tsunamis (MOST) model during the forecast model development. The test results presented in this report lend confidence that the model performs as developed and produces the same results when initiated within the forecast application in an operational setting as those produced by the researcher during the forecast model development. The test results assure those who rely on the Daytona Beach tsunami forecast model that consistent results are produced irrespective of system.

### C.2 Testing procedure

The general procedure for forecast model testing is to run a set of synthetic tsunami scenarios through the forecast system application and compare the results with those obtained by the researcher during the forecast model development and presented in the Tsunami Forecast Model Report. Specific steps taken to test the model include:

1. Identification of testing scenarios, including the standard set of synthetic events and customized synthetic scenarios that may have been used by the researcher(s) in developing the forecast model.
2. Creation of new events to represent customized synthetic scenarios used by the researcher(s) in developing the forecast model, if any.
3. Submission of test model runs with the forecast system, and export of the results from A, B, and C grids, along with time series.
4. Recording applicable metadata, including the specific version of the forecast system used for testing.
5. Examination of forecast model results from the forecast system for instabilities in both time series and plot results.

6. Comparison of forecast model results obtained through the forecast system with those obtained during the forecast model development.
7. Summarization of results with specific mention of quality, consistency, and time efficiency.
8. Reporting of issues identified to modeler and forecast software development team.
9. Retesting the forecast models in the forecast system when reported issues have been addressed or explained.

Synthetic model runs were tested on a DELL PowerEdge R510 computer equipped with two Xeon E5670 processors at 2.93 Ghz, each with 12 MBytes of cache and 32GB memory. The processors are hex core and support hyper threading, resulting in the computer performing as a 24 processor core machine. Additionally, the testing computer supports 10 Gigabit Ethernet for fast network connections. This computer configuration is similar or the same as the configurations of the computers installed at the Tsunami Warning Centers so the compute times should only vary slightly.

### C.3 Results

The Daytona Beach forecast model was tested with NOAA's tsunami forecast system version 3.2.

The Daytona Beach, Florida forecast model was tested with three synthetic scenarios (Table C1). Test results from the forecast system and comparisons with the results obtained during the forecast model development are shown numerically in Table C2 and graphically in Figures C1 to C3. The results show that the forecast model is stable and robust, with consistent and high quality results across geographically distributed tsunami sources and mega-event tsunami magnitudes. The model run time (wall clock time) was under 47 minutes for 12 hours of simulation time, and under 16 minutes for 4 hours. This run time is over the 10 minute run time for 4 hours of simulation time that satisfies time efficiency requirements.

Three synthetic events were run on the Daytona Beach forecast model. The modeled scenarios were stable for all cases tested, with no instabilities or ringing. Results show that the largest modeled height was 435.5 cm and originated in the Caribbean (ATSZ 48-57) source. Amplitudes greater than 100 cm were recorded for the two of three test sources. The smallest signal of 39.1 cm was recorded for the far field South Sandwich Islands (SSSZ 1-10) source. Direct comparisons, of output from the forecast tool with results from available development synthetic events, demonstrated that the wave patterns for the two Caribbean (ATSZ 48-57, ATSZ 38-47) sources are similar in shape, pattern and amplitude but do not match by eye. These discrepancies are mainly caused by different propagation databases used to provide the boundary conditions for model runs. Developed in 2008, the forecast model report shows the Daytona Beach model results based on an old tsunami propagation database, while the SIFT testing results in Appendix C reflect the tsunami propagation database that was updated in December of 2011. It is known that the new propagation database will lead to improvement of the model results. The wave pattern for the South Sandwich Islands (SSSZ 1-10) source does not look similar. The South Sandwich Islands

sources were incorrect and corrected in November of 2011 which would account for the difference.

Note: There were no maximum or minimum amplitudes listed in the report.

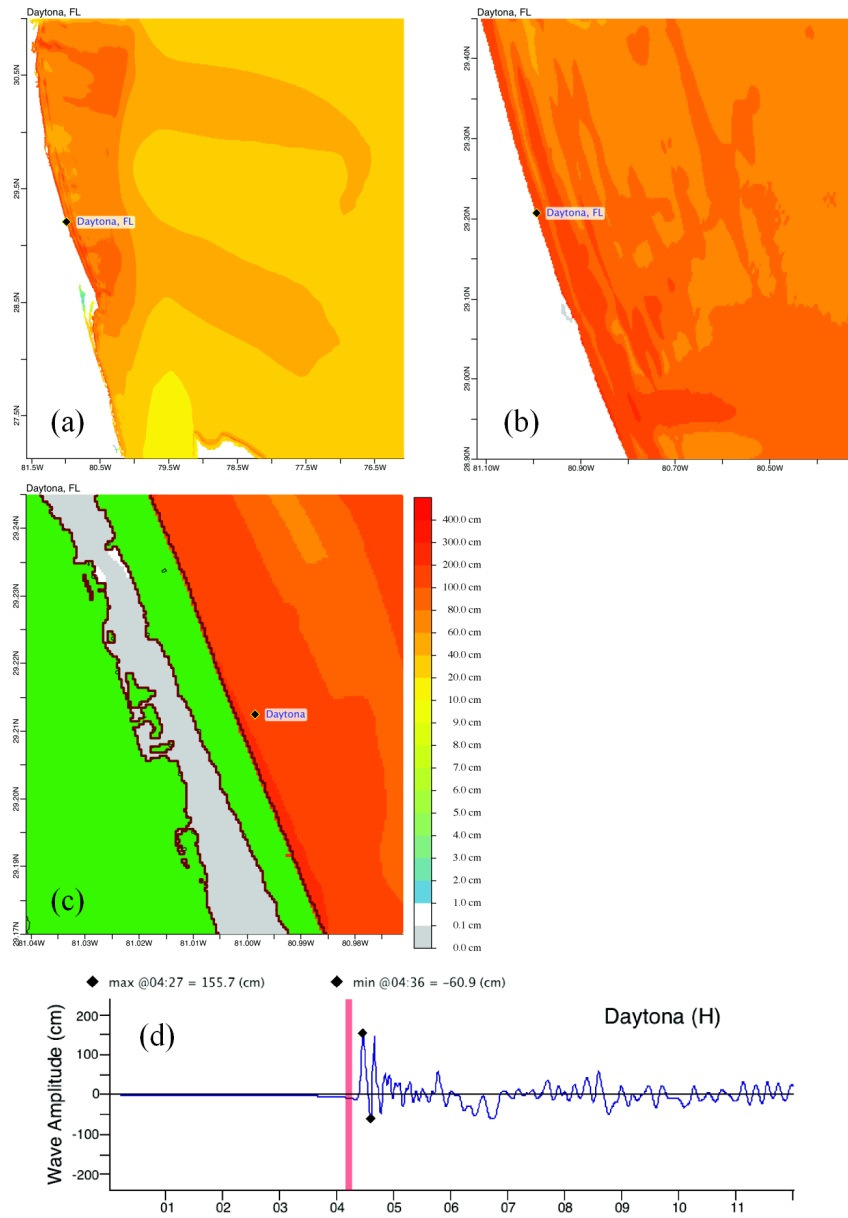


Figure C1: Testing results from the forecast model in scenario ATSZ 38-47: maximum water surface elevations in A-grid (a), B-grid (b), and C-grid (c), as well as time-series at the warning point (d).

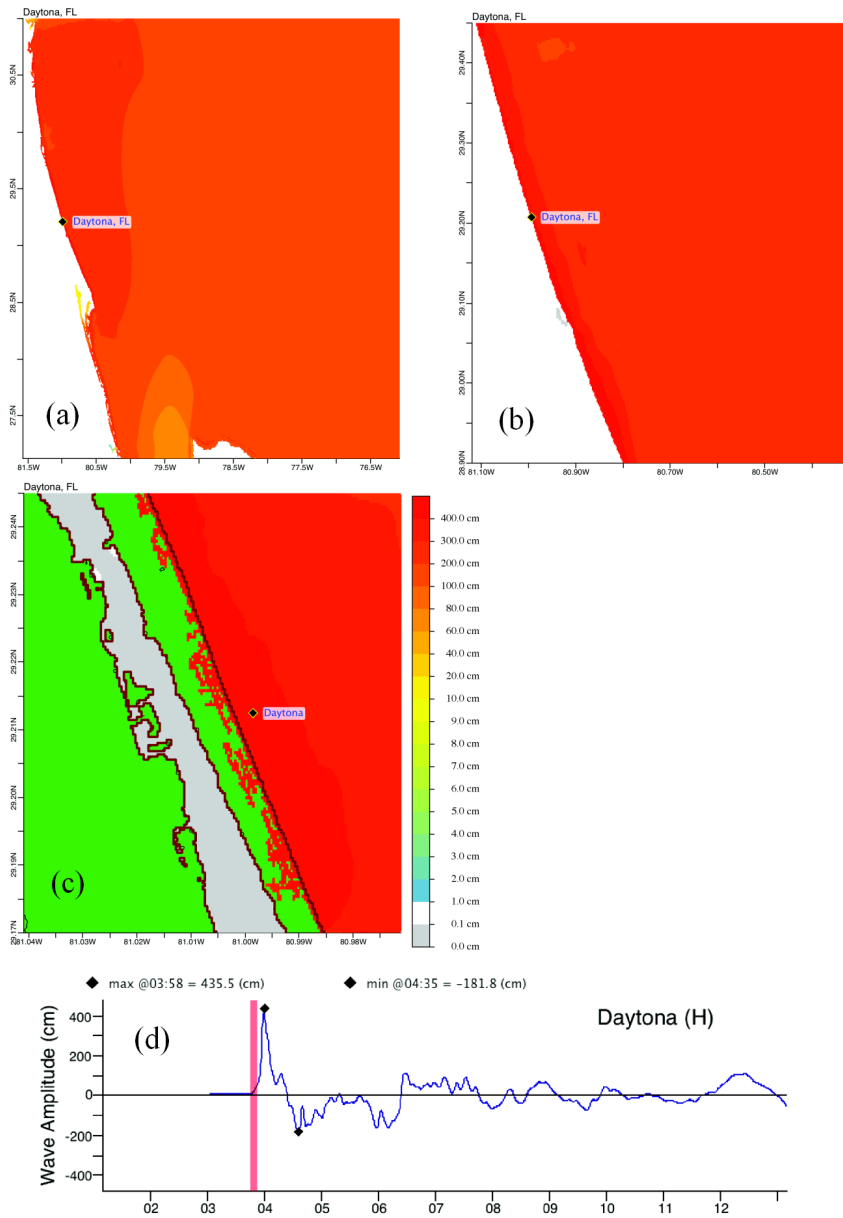


Figure C2: Testing results from the forecast model in scenario ATSZ 48-57: maximum water surface elevations in A-grid (a), B-grid (b), and C-grid (c), as well as time-series at the warning point (d).

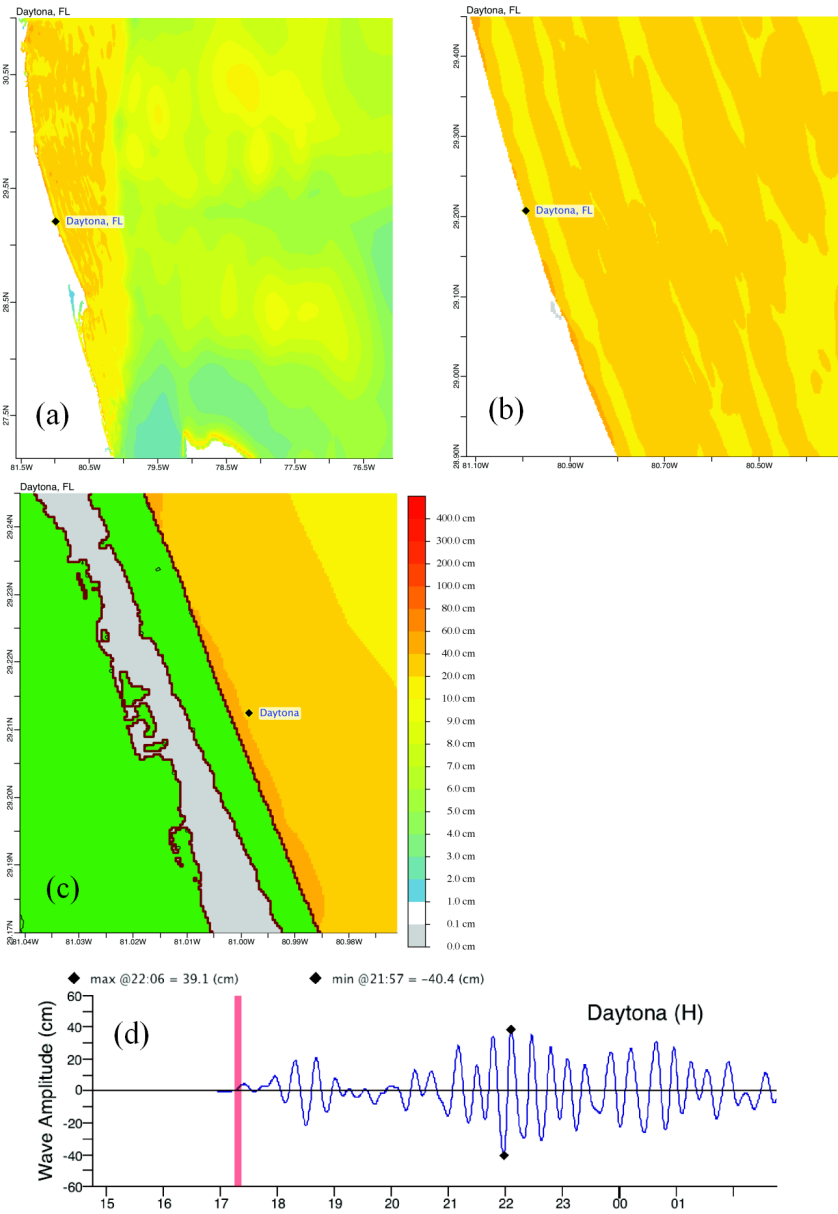


Figure C3: Testing results from the forecast model in scenario SSSZ 1-10: maximum water surface elevations in A-grid (a), B-grid (b), and C-grid (c), as well as time-series at the warning point (d).

Table C1: Run time of the Daytona Beach, Florida forecast model.

Model	Modeled Time [hrs]	Wall Time [min]	4-hour Time [min]	Space [Gb]	12-hour Space [Gb]
LW2-atsz38-47.02.IF_DYT	11.99	43.48	14.48	0.00	0.00
LW2-atsz48-57.03.IF_DYT	11.99	46.33	15.44	0.00	0.00
LW2-sssz1-10.03.IF_DYT	11.99	44.40	14.80	0.00	0.00

Table C2: Table of maximum and minimum amplitudes (cm) at the Daytona Beach, Florida warning point for synthetic and historical events tested using SIFT 3.2 and obtained during development.

Scenario Name	Source Zone	Tsunami Source	$\alpha$ [m]	SIFT Max (cm)	Development Max (cm)	SIFT Min (cm)	Development Min (cm)
<b>Mega-tsunami Scenarios</b>							
ATSZ 38-47	Caribbean	A38-A47, B38-B47	25	155.7	155.7	-60.9	-61.0
ATSZ 48-57	Caribbean	A48-A57, B48-B57	25	435.5	435.5	-181.8	-181.9
SSSZ 1-10	South Sandwich Islands	A1-A10, B1-B10	25	39.1	39.1	-40.4	-40.4